

Dynamics of Global Emission Permit Prices and Regional Social Cost of Carbon under Noncooperation ^{*}

Yongyang Cai[†] Khyati Malik[‡] Hyeseon Shin[§]

December 27, 2023

Abstract

We build a dynamic multi-region model of climate and economy with emission permit trading among 12 aggregated regions in the world. We solve for the dynamic Nash equilibrium under noncooperation, wherein each region adheres to the emission cap constraints following commitments outlined in the 2015 Paris Agreement. Our model shows that the emission permit price reaches \$749 per ton of carbon by 2050. We demonstrate that a regional carbon tax is complementary to the global cap-and-trade system, and the optimal regional carbon tax is equal to the difference between the regional marginal abatement cost and the permit price.

^{*}The authors have contributed equally to this work. We are grateful for comments and suggestions from the participants at PACE 2023 and the Heartland Workshop 2023. Cai acknowledges support from the National Science Foundation grant SES-1739909 and the USDA-NIFA-AFRI grant 2018-68002-27932. Shin acknowledges the support from the endowments of The Andersons Program in International Trade.

[†]Corresponding author. Department of Agricultural, Environmental and Development Economics, The Ohio State University. cai.619@osu.edu

[‡]Department of Agricultural, Environmental and Development Economics, The Ohio State University. malik.203@osu.edu

[§]Department of Agricultural, Environmental and Development Economics, The Ohio State University. shin.774@osu.edu

Keywords: Emission trading system, Paris Agreement, dynamic Nash equilibrium, integrated assessment model, carbon tax, social cost of carbon.

JEL Classification: C73, F18, Q54, Q58.

1 Introduction

Anthropogenic warming of our planet is projected to have disastrous consequences, from rising sea levels to increases in the frequency and intensity of extreme weather events (Arias et al., 2021). The first ever international effort to mitigate global emissions was undertaken in 1997 with the signing of the Kyoto protocol. More than two decades since the Kyoto protocol, global efforts to tackle climate change have failed, with the world experiencing accelerating rates of greenhouse gas emissions. The policy outlined in the 2015 Paris Agreement aimed to codify an objective of limiting climate change to a maximum of 2 degrees Celsius above pre-industrial levels. To accomplish this objective, the participating nations committed to Intended Nationally Determined Contributions (INDCs) specifying their emission mitigation goals. In November 2021, representatives of almost 200 countries met at Glasgow to renew their efforts in curbing climate change and approved the Glasgow Climate Pact with the overall aim of limiting the rise in global temperatures to 1.5 degrees Celsius through numerous actions.

Various market-based approaches to reduce emissions have been proposed, among which the most well-known are carbon tax regimes and emission trading systems (ETS). In a carbon tax regime, a tax is charged on firms for each unit of carbon emissions. The optimal global carbon tax rate is often determined at the global social cost of carbon (SCC), which is the present value of global climate damages incurred by an additional unit of carbon emissions (Nordhaus, 2017). On the other hand, in an emission trading or a cap-and-trade system, the maximum amount of emissions is fixed in an economy and agents can sell and purchase emission permits at the market price. Under the assumptions of complete information and no frictions, properly designed carbon tax

regimes and emission trading systems are argued to have equivalent outcomes (Nordhaus and Yang, 1996; Goulder and Schein, 2013). The ETS, however, is often considered a more efficient policy tool in practice, since it encourages agents that can reduce emissions at lower costs than others to undertake more emission reduction efforts (Nordhaus, 2017). In 2005, the European Union (EU) first adopted a legally binding emission trading system among the EU members, and as of the summer of 2023, the permit price stands at about 90 euros per ton of carbon.¹² Although a global-level ETS is not currently in place, it has emerged as a prominent potential mechanism to combat climate change, particularly since Article 17 of the Kyoto Protocol proposed emissions trading among countries.

In this study, we develop a dynamic multi-region model of climate and the economy under a hypothetical global ETS, and use it to project global prices of emission permits and the regional Social Cost of Carbon (SCC). In this integrated assessment framework, we formed 12 aggregated regions by grouping 198 countries around the world. Each region is allocated emission caps in accordance with the emission mitigation targets from the Paris Agreement and regional net zero commitments. Our main analysis involves solving a dynamic Nash equilibrium under noncooperation, where each region makes optimal dynamic decisions on emission abatement, emission permit purchases, and capital investment to maximize its social welfare given the optimal choices of other regions. Under the global ETS, regions with higher marginal abatement costs (MAC) are encouraged to purchase permits from the market to meet their emission cap constraints, whereas regions with lower MAC are incentivized to conduct more abatement and make profits by selling permits. The emission permit price is endogenously determined by annual supply and demand in the global permit market.

Our study makes four contributions. The first contribution of this study

¹Source of EU permit price: <https://tradingeconomics.com/commodity/carbon>.

²In addition to the EU ETS, other national or sub-national ETS have been implemented or are in the process of development, including in Canada, China, Japan, New Zealand, South Korea, Switzerland, and the United States. For a review of emission cap-and-trade systems in practice, see e.g., Schmalensee and Stavins (2017).

is a method to solve for the market equilibrium prices of emission permits under a global ETS. To the best of our knowledge, this is the first attempt to integrate an emission permit trading system with endogenous prices in a dynamic regional integrated assessment model. While prior research on the Regional Integrated Model of Climate and the Economy (RICE; Nordhaus, 2010) highlighted the importance of a multi-region ETS, it did not provide a solution for the market-clearing equilibrium permit price in a noncooperative setting. We present an algorithm for finding a Nash equilibrium solution in this context. Under the baseline emission cap scenario based on the Paris Agreement and the regional net zero commitments, our simulation results show that the oversupply of global permits in the initial decade results in zero permit prices, but by 2050, the emission permit price can reach up to \$749 per ton of carbon. Furthermore, we show that regions such as the United States, India and the EU become major emission permit buyers, and other regions such as Russia and China become permit suppliers.

The second contribution is demonstrating, both theoretically and numerically, that regional optimal taxes can be internally implemented under the global ETS. While carbon taxes and ETS have often been considered as potentially interchangeable policies, we show that within the global ETS framework, the social planner of each region can introduce a carbon tax as a complementary policy tool to achieve its optimal level of net emissions. The necessity of a carbon tax arises from the discrepancy in optimal net emissions between the social planner's choice and the market outcome under the ETS. When optimal net emissions from the social planner's perspective are strictly positive, the regional optimal carbon tax is equal to the difference between the regional MAC and the global permit price under the noncooperative Nash equilibrium with the ETS. We also numerically verify that the regional optimal carbon tax is equal to the regional SCC when net emissions are strictly positive.

The third contribution is that our model's results are based on newly calibrated parameters and regional emission cap pathways under the Paris Agreement, enhancing the accuracy and relevance of our findings. We calibrate our model by fitting it to historical data and the recent predicted

trends of regional climate damage, regional GDP, regional abatement costs, and population projections based on the Shared Socioeconomic Pathway 2 (SSP2; Samir and Lutz, 2017), also known as the “Middle-of-the-Road” scenario. Besides this calibration, our model uses a stylized but stable climate system, called the Transient Climate Response to Emissions (TCRE; Matthews et al., 2009), which assumes that increases in the global averaged atmospheric temperature have a nearly linear functional dependence on cumulative carbon emissions. We show that this temperature system can be calibrated to match closely with the various Representative Concentration Pathways (RCPs; Meinshausen et al., 2011). Due to its simplicity and effectiveness, the TCRE scheme has found application in recent economic analyses, as evidenced by studies such as Brock and Xepapadeas, 2017; Dietz and Venmans, 2019; Mattauch et al., 2020; Barnett et al., 2020. Moreover, Dietz et al. (2021) show that the TCRE scheme does not lead to a large difference in economic analysis with the seminal DICE framework (Nordhaus, 2017), compared to other more complicated climate systems.

Our final contribution is a comprehensive comparative analysis of the roles played by cooperation, emission caps, and the global ETS. Our simulations reveal that global cooperation leads to significantly lower emissions and lower temperature rises. We also find that the global ETS leads to higher emissions under noncooperation, because regions with binding emission caps can purchase permits from regions with less restrictive caps, exploiting the excessively abundant emission permits in the first decade. This implies that it is important to maintain a stringent emission cap at the global level to make the ETS work efficiently. Moreover, we show that a stricter emission cap leads to a higher permit price and smaller regional SCCs for every region. For example, if all the regions achieve net zero emissions in 2050, the emission permit price can reach up to \$1,538 per ton of carbon by 2049. However, even with this strict emission restriction, the global temperature is still projected to rise by 1.64 degrees Celsius by the end of this century. These findings suggest that achieving the global target of limiting the temperature rise to 1.5 degrees Celsius requires even stronger emission commitments than those outlined in the

Paris Agreement. We also find that under cooperation between the regions, the regional SCC is higher for a developed region compared to a developing one. That is, there are higher carbon taxes in developed regions under cooperation compared to developing regions because the marginal utility of consumption is higher in developing regions. Global aggregate welfare will be higher if developed regions can contribute more to mitigating emissions, thus reducing climate damages in developing regions. In the noncooperative setting, the regional SCCs of the developed and the developing regions are comparable.

In the literature, the ETS has garnered attention as a promising mechanism for mitigating global emissions, along with carbon taxes, but there have been relatively limited attempts to comprehensively analyze the ETS as a potential tool for global climate policy. One closely relevant study is Carbone et al. (2009), which builds a computable general equilibrium model of the world, incorporating countries' endogenous participation in an ETS and allocation of emission permits, and solves for the equilibrium permit price. In contrast to our work, their study is based on a static setting, so it does not address the critical dynamic aspects of climate change, and lacks a connection with emission abatement decisions. Fischer and Springborn (2011) is another relevant work that constructs a dynamic stochastic general equilibrium model to compare the outcomes of the emission cap and tax policies, but their model does not consider emission trading between regions.

More broadly, a series of recent studies have examined ETS from various perspectives. Some studies have focused on empirically analyzing the regional emission trading markets currently in practice, such as the EU ETS or China ETS (Fuss et al., 2018; Hitzemann and Uhrig-Homburg, 2018; Borenstein et al., 2019; Goulder et al., 2022; Perino et al., 2022). Others analyze the efficiency gains from integrating regional ETS (Habla and Winkler, 2018; Doda et al., 2019; Holtmark and Weitzman, 2020; Holtmark and Midttømme, 2021), or compare the emission permit allocation methods between auctioning and free allocation (Goulder et al., 2010). While a global ETS is not yet in place, it is expected to offer multiple benefits compared to a global carbon tax. In an international ETS, emission permits will be traded globally with one price

for all nations based on market forces, which may alleviate the problem of carbon leakage (Fowlie et al., 2016). An international ETS requires little governmental interference, and will help regions to maintain their emission target commitments and thereby contribute towards controlling the global temperature rise. On the other hand, a uniform global carbon tax regime is practically challenging. This paper therefore contributes to the literature by proposing a global ETS with endogenous permit prices and associated regional carbon taxes under various emission caps.

Our model framework is closely related to the recent developments in integrated assessment models (IAMs), which aim to capture the interaction between economic growth and climate systems under cooperation and noncooperation. A seminal work is the RICE model (Nordhaus and Yang, 1996; Nordhaus, 2010), which extends the global DICE model (Nordhaus, 2014) by building a multi-region dynamic framework. Nordhaus (2010) computes carbon prices under a cooperative model where global welfare is maximized with weights applied on regional utilities. Following the RICE model, a group of studies have explored climate policy in a dynamic multi-region context under cooperation and noncooperation. For instance, Hambel et al. (2021) extend the RICE framework by integrating endogenous international trade under noncooperation and provide a closed-form analytical solution for the regional SCCs, under certain model assumptions. van der Ploeg and de Zeeuw (2016) and Jaakkola and Van der Ploeg (2019) focus on stochastic components of the model, such as climate tipping points or technological breakthroughs, comparing the results under different levels of cooperation. Cai et al. (2023) build a dynamic IAM for two economic regions (North and Tropic/South) to compute regional SCCs under cooperation and noncooperation. Nonetheless, none of these works examine the dynamics of an international ETS with an endogenous market price of emission permits under a noncooperative setting. Our study builds on the concept of regional SCCs defined in van der Ploeg and de Zeeuw (2016) and Cai et al. (2023) and provides a comprehensive analysis of regional SCCs and their relation with the global ETS in a multi-region dynamic framework under noncooperation.

2 A Dynamic Regional Model of Climate and the Economy with an ETS

This section introduces a dynamic regional model of climate and the economy that integrates a global ETS between 12 aggregated regions. Our model framework extends the RICE model (Nordhaus and Yang, 1996; Nordhaus, 2010) by incorporating the global ETS in a dynamic setting and the TCRE climate system with annual time steps. The main objective of this study is to present a potential dynamic path of carbon emission prices in a noncooperative environment where each region aims to maximize its own social welfare by choosing the optimal amount of emission abatement, emission permits purchased from the global permits market, and the amount of its consumption. The model is based on the assumption that future regional emissions are strictly constrained by the emission caps set by the commitments under the Paris Agreement and net zero emissions targets.

The macroeconomic framework of our model employs a multi-regional representation of the Ramsey growth model. We follow the RICE model and assume that the world consists of 12 aggregated regions: the United States (US), the EU, Japan, Russia, Eurasia, China, India, Middle East (MidEast), Africa, Latin America (LatAm), Other High-Income countries (OHI) and other non-OECD Asia (OthAs).³ Each region is indexed by $i \in \mathcal{I}$, where \mathcal{I} is the set of regions. Time is discrete, with annual time steps indexed by $t = 0, 1, 2, \dots$, where the initial time period is the year 2020. All regions are forward-looking with complete information.

2.1 Emissions

The total industrial carbon emissions before abatement, in gigatonnes of carbon (GtC), is assumed to be proportional to the gross output for region i at time t :

$$E_{i,t}^{\text{Total}} = \sigma_{i,t} Q_{i,t}, \quad (1)$$

³See Appendix 1 A.2 for the full list of countries and regional aggregation.

where $Q_{i,t}$ is the gross output, and $\sigma_{i,t}$ is the exogenous carbon intensity, calibrated from the projections of GDP and emissions in Ueckerdt et al. (2019). The amount of emissions abated by each region, $E_{i,t}^A$, is expressed as a fraction of the total industrial emissions, with an emission control rate $\mu_{i,t} \in [0, 1]$. That is,

$$E_{i,t}^A = \mu_{i,t} \sigma_{i,t} Q_{i,t}. \quad (2)$$

Thus the net emissions, $E_{i,t}$, becomes

$$E_{i,t} = E_{i,t}^{\text{Total}} - E_{i,t}^A. \quad (3)$$

We consider a global ETS, or a cap-and-trade system, in which each region is provided with an emission allowance and can trade emission permits with other regions. Regions with net emissions exceeding the emission caps can purchase emission permits from other regions. Regions with emissions below their allowance can sell their emission permits to others. The emission cap constraint is represented by

$$E_{i,t} - E_{i,t}^P \leq \overline{E}_{i,t}, \quad (4)$$

where $\overline{E}_{i,t}$ is the emission cap assigned to region i at time t , and $E_{i,t}^P$ denotes the amount of emissions traded with other regions. Note that $E_{i,t}^P > 0$ indicates that region i is a net buyer of emission permits at time t , while $E_{i,t}^P < 0$ implies region i is a net seller of emission permits at time t . In a model that does not consider emission permit trade, we simply apply $E_{i,t}^P = 0$ for all i and t . The Paris Agreement establishes upper limits for net emissions to ensure that the increase in global temperature remains well below 2 degrees Celsius above preindustrial levels by the end of this century.

2.2 Climate System

The global average temperature rises as carbon emissions accumulate in the atmosphere. We follow the TCRE climate system and assume that the global

average temperature increase above the pre-industrial level is approximately proportional to cumulative global emissions \mathcal{E}_t , i.e.,

$$T_t = \zeta \mathcal{E}_t, \quad (5)$$

where the cumulative emissions at 2020, \mathcal{E}_0 , is chosen such that the initial global mean temperature T_0 is 1.2 degrees Celsius above the pre-industrial level. Here $\zeta = 0.0021$ is the contribution rate of CO₂ equivalent to temperature, calibrated with the projections of emissions and temperatures in the four Representative Carbon Concentration Pathways (RCPs): RCP 2.6, RCP 4.5, RCP 6.0, and RCP 8.5 (Meinshausen et al., 2011). Figure A.1 in Appendix A.3 shows that the calibrated TCRE climate system can match all four RCP temperature pathways using their associated RCP emission pathways. Cumulative global emissions evolve according to

$$\mathcal{E}_{t+1} = \mathcal{E}_t + \sum_{i \in \mathcal{I}} E_{i,t}. \quad (6)$$

2.3 Economic System

A representative consumer in region i has a power utility per period as follows:

$$u(c_{i,t}) = \frac{c_{i,t}^{1-\gamma}}{1-\gamma}, \quad (7)$$

where $c_{i,t}$ is per capita consumption and γ is the inverse of intertemporal elasticity of substitution. We follow DICE-2016R Nordhaus (2017) and set $\gamma = 1.45$.

The production technology follows a Cobb-Douglas function of capital and labor inputs. The gross output (in trillion USD), or pre-damage output, $Q_{i,t}$, is given by

$$Q_{i,t} = A_{i,t} K_{i,t}^\alpha L_{i,t}^{1-\alpha}, \quad (8)$$

where $K_{i,t}$ is capital stock, $L_{i,t}$ is labor, and $\alpha = 0.3$ (following Nordhaus

(2017)) is the elasticity of gross output with respect to capital. The total factor productivity $A_{i,t}$ is assumed to follow an exogenous and deterministic time-varying trend, which is calibrated with the no-climate-impact GDP projections in Burke et al. (2018). Labor $L_{i,t}$ is also assumed to follow the exogenous population path of region i from the SSP2 scenario (Samir and Lutz, 2017).

We denote $Y_{i,t}$ as the output net of damages induced by climate changes:

$$Y_{i,t} = \frac{1}{1 + \pi_{1,i}T_t + \pi_{2,i}T_t^2}Q_{i,t}, \quad (9)$$

where T_t is the global average temperature increase in degrees Celsius above the preindustrial level. We calibrate the climate damage parameters based on the projections of GDP loss in Kahn et al. (2021). We follow DICE and assume emission abatement cost is

$$\Phi_{i,t} = b_{1,i,t}\mu_{i,t}^{b_{2,i}}Q_{i,t},$$

where $b_{1,i,t} = (b_{1,i} + b_{3,i}\exp(-b_{4,i}t))\sigma_{i,t}$. We calibrate the abatement cost parameters, $b_{1,i}$, $b_{2,i}$, $b_{3,i}$, and $b_{4,i}$, by exploiting the projections under different carbon tax scenarios in Ueckerdt et al. (2019), from which we recover the marginal abatement costs and calibrate the parameters we need.

The total consumption of each region under the ETS is obtained by

$$c_{i,t}L_{i,t} = Y_{i,t} - I_{i,t} - \Phi_{i,t} - m_tE_{i,t}^P, \quad (10)$$

where $I_{i,t}$ is investment and m_t is the market price of carbon emission permits. The cost of purchasing emission permits from other regions results in reduced consumption, while selling emission permits increases consumption. The capital stock evolves according to the standard neoclassical growth model:

$$K_{i,t+1} = (1 - \delta)K_{i,t} + I_{i,t}, \quad (11)$$

where $\delta = 0.1$ is the rate of depreciation of capital stock. We assume that the

emission trading market clears in each period. That is,

$$\sum_{i \in \mathcal{I}} E_{i,t}^P = 0, \quad (12)$$

for each time period t .

3 Solving for the Equilibrium

Based on the model components introduced in Section 2, we now define equilibrium under cooperative and noncooperative models in the ETS. These two extreme cases place bounds on what we would observe in a real world scenario.

3.1 The Cooperative and the Noncooperative Model

In the cooperative model, all regions work together to maximize their combined welfare. More specifically, the objective function is to maximize the overall sum of discounted social utility across all regions as follows:

$$\max_{c_{i,t}, E_{i,t}^P, \mu_{i,t}} \sum_{t=0}^{\infty} \sum_{i \in \mathcal{I}} \beta^t u(c_{i,t}) L_{i,t} \quad , \quad (13)$$

where β is the discount factor. We follow DICE-2016R (Nordhaus, 2017) and set $\beta = 0.985$. Note that under cooperation there is no market equilibrium permit price, so we assume permit prices follow an exogenous path. Therefore, we define the cooperative model equilibrium given an exogenous path of permit prices.

DEFINITION: Given the initial capital and cumulative global emissions, $\{K_{i,0}, \mathcal{E}_0 : i \in \mathcal{I}\}$, and the exogenous paths of emission caps and permit prices, $\{\bar{E}_{i,t}, m_t : i \in \mathcal{I}, t \geq 0\}$, the dynamic equilibrium for the cooperative model is a sequence of quantities $\{c_{i,t}, E_{i,t}^P, \mu_{i,t}, K_{i,t}, \mathcal{E}_t, T_t : i \in \mathcal{I}, t \geq 0\}$ that solve the maximization problem (13) subject to equations (7)-(12).

In the noncooperative model, individual regions maximize their own lifetime social welfare, which represents another extreme but relatively more realistic perspective. The maximization problem for each region i is defined as

$$\max_{c_{i,t}, E_{i,t}^P, \mu_{i,t}} \sum_{t=0}^{\infty} \beta^t u(c_{i,t}) L_{i,t}. \quad (14)$$

DEFINITION: Given the initial capital and cumulative global emissions, $\{K_{i,0}, \mathcal{E}_0 : i \in \mathcal{I}\}$, and the exogenous paths of emission caps $\{\bar{E}_{i,t} : i \in \mathcal{I}, t \geq 0\}$, the dynamic Nash equilibrium for the noncooperative model is a sequence of quantities $\{c_{i,t}, E_{i,t}^P, \mu_{i,t}, K_{i,t}, \mathcal{E}_t, T_t : i \in \mathcal{I}, t \geq 0\}$ and prices $\{m_t : t \geq 0\}$ that simultaneously solve the maximization problem (14) for all regions subject to equations (7)-(12).

The optimal solution for this dynamic multi-region model involves three choice problems. First, as in the standard Ramsey-type growth model, each region faces an intertemporal choice problem in which there is a trade-off between current consumption and future consumption. Each region may sacrifice present consumption to make investments, which can contribute to higher consumption in the future. Second, the intertemporal choice problem is further compounded by climate damages. Current production increases the global temperature, which subsequently lowers future productivity. Since emissions abatement has positive externalities, a region's returns from abatement efforts may not be large enough to offset the cost of abatement. Therefore, the optimal solution of each region is highly dependent on the choices made by other regions. Lastly, the ETS allows each region to choose between purchasing emission permits from the market and undertaking further abatement. The ETS promotes efficient abatement globally by encouraging regions with better abatement technology or capacity (thus, with lower abatement cost) to conduct more abatement, and regions with less efficient abatement technology to purchase permits from other regions.

3.2 The Algorithm for the Noncooperative Model

Obtaining the optimal solution of the dynamic model involving multiple regions under noncooperation is challenging. In particular, finding an equilibrium solution for the emission permit prices that satisfies the optimality conditions for each region as well as the market clearing condition poses significant computational challenges. While several studies have incorporated emission prices in their models, no study has successfully solved for the emission permit price in a noncooperative context.

Here we outline the algorithm we develop to obtain the optimal solution for our model. Since $\gamma = 1.45$ implies utilities of per capita consumption have negative values and that long-run per capita consumption will be large, the long-run per-capita utility has a small magnitude. Together with the discount factor $\beta = 0.985$, the discounted utilities after 300 years are nearly zero and have little impact on the solution in the first 100 years. Thus, we can transform the infinite horizon models to finite horizon models, where region i 's social welfare is rewritten as

$$\sum_{t=0}^{299} \beta^t u(c_{i,t}) L_{i,t} + \beta^{300} u\left(\frac{0.75Y_{i,300}}{L_{i,300}}\right) \frac{L_{i,300}}{1-\beta}.$$

Here the second term is an approximation of the sum of discounted utility from time $t = 300$ to infinity, assuming that consumption at any $t \geq 300$ is identical to 75 percent of the output at $t = 300$ and that the exogenous population after 300 years stays at its value at $t = 300$. The algorithm to solve the noncooperative model is as follows:

Step 1. Initialization. Give an initial guess of permit prices $\{m_t^0 : t \geq 0\}$ and solve the cooperative model with emission cap and trade. The optimal net emissions and the amount of emission permits traded with the other regions are denoted as $\{E_{i,t}^0, E_{i,t}^{P,0} : t \geq 0\}$, for each region i . Iterate through steps 2, 3 and 4 for $j = 0, 1, \dots$, until convergence.

Step 2. Maximization Step. Solve the maximization problem (14) without the market clearing condition (12) for each region. Given the permit

prices $\{m_t^j : t \geq 0\}$, we solve the optimization problem (14) without the market clearing condition (12) for region 1, where we fix the other regions' net emissions at $\{E_{i,t}^j : i = 2, \dots, 12, t \geq 0\}$. We then obtain region 1's optimal solution, where the optimal net emissions and the amount of emission permits traded with the other regions are denoted as $\{E_{1,t}^*, E_{1,t}^{P,j+1} : t \geq 0\}$. Similarly, we obtain $\{E_{i,t}^*, E_{i,t}^{P,j+1} : t \geq 0\}$ for regions $i = 2, \dots, 12$.

Step 3. *Update the emission permit prices and net emissions.* After solving for the optimization problem of all regions, update the permit prices and net emissions as

$$\begin{aligned} m_t^{j+1} &= m_t^j \exp \left(\omega \sum_{i \in \mathcal{I}} E_{i,t}^{P,j+1} \right), \\ E_{i,t}^{j+1} &= \omega E_{i,t}^* + (1 - \omega) E_{i,t}^j, \quad \forall i \in \mathcal{I}, \end{aligned}$$

where $\omega = 0.1$ is a weight parameter and $\sum_{i \in \mathcal{I}} E_{i,t}^{P,j+1}$ is the net quantity of traded emission permits.

Step 4. *Check the convergence criterion.* Check if $m_t^{j+1} \simeq m_t^j$, $E_{i,t}^{j+1} \simeq E_{i,t}^j$, and $E_{i,t}^{P,j+1} \simeq E_{i,t}^{P,j}$ for every region i and $t \geq 0$. If so, stop the iteration. Note that $m_t^{j+1} = m_t^j$ implies that the market clearing condition (12) holds at the solution.

This algorithm embodies the concept of market equilibrium. When there is a positive net quantity of traded emission permits in the market, indicating excess demand, we increase the permit prices. Conversely, when there is a negative net quantity of traded emission permits, indicating excess supply, we lower the permit prices. This mechanism ensures that the market reaches a balance between supply and demand, and thus the market clears. Furthermore, this algorithm guarantees that each region obtains its optimal solution and reaches an equilibrium state. In other words, no region has the incentive to deviate from the Nash equilibrium for the noncooperative model solution. Note that the equilibrium of the noncooperative model is an open-loop Nash

equilibrium (OLNE), which provides a solution path over time depending on the initial state.

4 SCC, MAC, and the Optimal Carbon Tax

In this section, we first define the regional social cost of carbon (SCC) and marginal abatement cost (MAC) and explain how the optimal carbon tax can be introduced together with the global ETS, in relation to the SCC and MAC.

4.1 SCC and MAC

The social cost of carbon (SCC), a central concept in the climate change literature, is widely used to quantify the monetary value of climate damages induced by an additional unit of carbon emissions. While the SCC is often calculated in a global social planner's problem (e.g., the DICE model), we consider the SCC for each region. Similar to van der Ploeg and de Zeeuw (2016) and Cai et al. (2023), we define the cooperative SCC of a region as the marginal rate of substitution between global emissions and regional capital as follows:

$$\text{SCC}_{i,t}^{\text{Coop}} = \frac{-1,000(\partial V_t^{\text{Coop}} / \partial \mathcal{E}_t)}{\partial V_t^{\text{Coop}} / \partial K_{i,t}}, \quad (15)$$

for region i , where V_t^{Coop} is the value function of the cooperative model at time t , depending on the state variables $\{K_{i,t}, \mathcal{E}_t : i \in \mathcal{I}\}$; that is,

$$V_t^{\text{Coop}}(K_{1,t}, \dots, K_{12,t}, \mathcal{E}_t) = \max_{c_{i,s}, E_{i,s}^P, \mu_{i,s}} \sum_{s=t}^{\infty} \beta^t \sum_{i=1}^{12} u(c_{i,s}) L_{i,s}.$$

Similarly, the noncooperative SCC of a region is defined as

$$\text{SCC}_{i,t}^{\text{OLNE}} = \frac{-1,000(\partial V_{i,t}^{\text{OLNE}} / \partial \mathcal{E}_t)}{\partial V_{i,t}^{\text{OLNE}} / \partial K_{i,t}}, \quad (16)$$

where

$$V_{i,t}^{\text{OLNE}}(K_{1,t}, \dots, K_{12,t}, \mathcal{E}_t) = \max_{c_{i,s}, E_{i,s}^P, \mu_{i,s}} \sum_{s=t}^{\infty} \beta^t u(c_{i,s}) L_{i,s},$$

for each region i under the OLNE.

Since our cumulative global emissions are measured in gigatonnes of carbon (GtC) and capital is measured in trillions of USD, our SCC is measured in 2020 USD per ton of carbon. To compute the regional SCC in the cooperative or the noncooperative model, it is equivalent to replace the numerator in equation (15) or (16) with the shadow price of the transition equation of cumulative global emissions (6) at time t , and replace the denominator with the shadow price of the regional capital transition equation (11) for each region.

It should be emphasized that our concept of the regional SCC differs from the definition in Nordhaus (2017) and Ricke et al. (2018). Note that, for the global SCC, the marginal rate of substitution between global emissions and global capital (or consumption) is equivalent to the present value of future global climate damages from an additional unit of global emissions released in the current period. In this regard, it has been well understood in the literature that the global SCC can be used as the optimal global carbon tax. However, in Nordhaus (2017) and Ricke et al. (2018), their regional SCC is defined as the present value of future climate damages in a region resulting from an additional unit of global emissions released in the current period. Such definition implies that their regional SCC is the regional contribution to the global SCC, i.e., the sum of their regional SCCs over all regions is the global SCC. This does not make sense in the context of carbon tax.

We define the regional noncooperative SCC as the marginal rate of substitution between cumulative global emissions and regional capital under the OLNE. With our definition, the regional noncooperative SCC is equal to the optimal regional carbon tax under noncooperation when the regional net emissions is not binding at zero (i.e., the regional emission control rate is less than one), or is larger than the optimal regional carbon tax when the regional net emissions is binding at zero. This pattern is consistent with the relation between the global SCC and the optimal global carbon tax as shown in Cai et al.

(2017) and Cai and Lontzek (2019). Similarly, the regional cooperative SCC in our definition is equal to the optimal regional carbon tax under cooperation, when the regional net emissions is not binding at zero and the exogenous emission permit price is zero (or there is no ETS). However, when the exogenous emission permit price is nonzero, the regional cooperative SCC is not equal to the optimal regional carbon tax under cooperation, because the ETS can be used as a means for transferring capital between regions to improve the global welfare under cooperation. For instance, a developed region can purchase a large amount of permits from a developing region even when its net emissions has been below its emission cap.

The marginal abatement cost (MAC) is another important concept that captures the additional cost incurred due to an increase in emission abatement. From our model equation (2), the total abatement cost is $TAC_{i,t} = b_{1,i,t} \mu_{i,t}^{b_{2,i}} Q_{i,t}$, in trillions of USD. Thus, the MAC, in 2020 USD per ton of carbon, is obtained as follows

$$MAC_{i,t} = 1,000 \left(\frac{\partial TAC_{i,t}}{\partial E_{i,t}^A} \right) = 1,000 \left(\frac{b_{1,i,t} b_{2,i} \mu_{i,t}^{b_{2,i}-1}}{\sigma_{i,t}} \right).$$

When there is no ETS, it is well known that the optimal carbon tax is equal to the MAC. This equality has been often used in the literature (e.g., Nordhaus, 2014; Cai et al., 2017; Cai and Lontzek, 2019). However, in the presence of the ETS, the equality does not hold as firms can purchase or sell emission permits instead of abatement.

4.2 Optimal Carbon Tax under the ETS

In this subsection, we discuss the relationship between the MAC and carbon taxation under the global ETS. While carbon taxes and ETS have often been considered as substitutable policies, we show that each region can internally choose an optimal carbon tax under the global ETS as a complementary policy tool to obtain the optimal level of net emissions. Before we discuss the optimal carbon tax, the mechanism behind the emission permit buyer and seller

regions needs to be understood. Here we drop the region and time indices for simplicity.

First of all, the relationship between the optimal net emission (E^*) and emission cap (\bar{E}) determines whether a region becomes a permit buyer or seller. A region becomes a permit buyer if its optimal net emission is greater than the emission cap, i.e., $E^* > \bar{E}$. It follows that the emission quantity of ($E^* - \bar{E}$) becomes the optimal quantity of permits purchased and ($E^{\text{Total}} - E^*$) is the optimal emission abatement. On the other hand, a region becomes a permit seller if its optimal net emission is lower than its emission cap, i.e., $E^* < \bar{E}$, with the optimal quantity of permits sold captured by ($\bar{E} - E^*$). Note that this is the optimal solution from the perspective of each region's social planner.

One issue arises when the social planner of each region cannot internally force its firms—the actual emission producers in the economy—to obtain the social planner's optimal net emission level. We assume that the social planner uses carbon taxation as the policy instrument to fix the inconsistency between the optimal net emissions of the regional social planner and the firms. Let us consider a representative firm in each region that produces emissions and faces the MAC function and the emission cap of the region. We assume that the representative firm is myopic and maximizes its profit in each period, thus it does not consider the dynamic optimization problem of the social planner. Given the total emissions, E^{Total} , the representative firm's profit maximization problem is equivalent to choosing its optimal level of net emissions to minimize its total cost associated with emissions (i.e. the abatement cost and revenue or expenditures from emission permit purchases or sales).⁴

Figure 1 depicts the relationship between emissions, permit prices, the carbon tax, and the MAC for buyer and seller regions. In Figure 1, the MAC curve is a decreasing function of net emissions (E),⁵ which reaches zero when

⁴It is worth mentioning that a region's total emissions is proportional to its GDP, which, in turn, is determined by capital and the exogenous path of population size. Considering that the current level of capital is determined in the previous period, total emissions can be considered as exogenously given from the perspective of the single-period myopic firm.

⁵Substituting $E^A = E^{\text{Total}} - E$ from equation (3) into the MAC, it follows that $\text{MAC}_{i,t} =$

net emissions equals total emissions (E^{Total}). That is, the higher the emission abatement, the smaller the net emissions, resulting in a higher MAC. The market equilibrium price of emission permits is given at m . Then in the absence of a carbon tax, there is a corresponding cut-off level of net emissions, E^m , above which conducting the emission abatement is more cost-effective, and below which purchasing emission permits from the permit markets is cheaper.

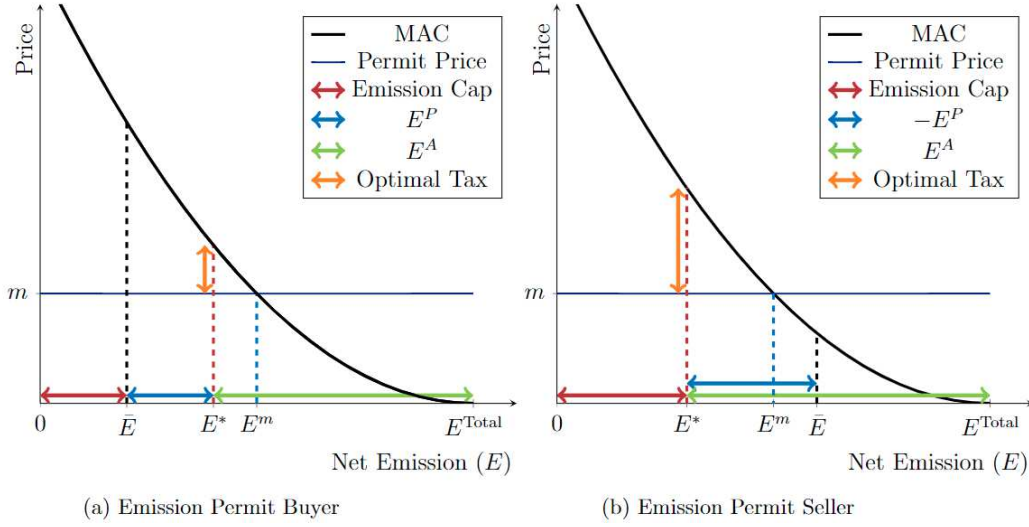


Figure 1: The optimal carbon tax in emission permit buyer and seller regions.

In the case of a permit buyer region (the left panel of Figure 1), if there is no carbon tax, when the firm's net emission is smaller than E^m , then its MAC is larger than the permit price m , so the firm has an incentive to purchase a quantity of $(E^m - \bar{E})$ emission permits and reduce its abatement effort until its net emissions become E^m . Conversely, in a permit seller region (the right panel of Figure 1), if there is no carbon tax, when the firm's net emission is smaller than E^m , it is more profitable for the firm to reduce its abatement effort until its net emissions reach E^m and then sell a quantity of $(\bar{E} - E^m)$ emission permits. That is, in the absence of a carbon tax, the social planner's optimal net emission level, E^* , may not align with the optimal choice of firms

$$1,000 \left(\frac{b_{1,i,t} b_{2,i}}{\sigma_{i,t}} \right) \left(\frac{E_{i,t}^{\text{Total}} - E_{i,t}}{\sigma_{i,t} Q_{i,t}} \right)^{b_{2,i} - 1}.$$

within each region, E^m , regardless of whether the region is a permit buyer or seller. Note that it is impossible for the firm's net emissions to be larger than E^m (i.e., its MAC to be smaller than m), because the firm as a buyer is not willing to purchase emission permits at a price m that exceeds its MAC (it would instead reduce its costs via more abatement), and the firm as a seller would prefer to reduce its net emissions so it can sell more permits at m to increase its profits. This is also verified in our simulation results later on.

We now show that a regional carbon tax can serve as a supplementary policy for the representative firm to reach the social planner's optimal net emissions at E^* . Assume that the social planner levies a tax on the firm of τ per unit of net emissions. Given the total emissions, E^{Total} , the cost minimization problem of the representative firm that faces this carbon tax under the global ETS is as follows:

$$\min_{E \geq 0} \quad \tau E + (E - \bar{E})m + \int_E^{E^{\text{Total}}} \text{MAC}(E') dE'. \quad (17)$$

The first term of the objective function is the total tax on net emissions, the second term is the cost from purchasing permits at the price m (or the profit from selling permits), and the third term is the total abatement cost for reducing emissions by the amount $(E^{\text{Total}} - E)$. The above cost minimization problem holds for both emission permit buyer and sellers. For simplicity, we assume that emissions cannot be negative in our model.

From the Karush-Kuhn-Tucker conditions of (17), the solution to the optimal net emissions of a firm leads to the following relationship between the carbon tax, the MAC, and the permit price:

$$\tau = \text{MAC}(E^*) - m, \quad (18)$$

when $E^* > 0$. Importantly, it implies that for the representative firm to attain the optimal net emission level E^* , the social planner can impose an internal carbon tax at $\text{MAC}(E^*) - m$, which is also equal to the regional SCC in our definition when $E^* > 0$. In other words, the optimal regional carbon tax is

endogenously determined by the gap between the MAC of a region and the market price of emission permits. It aligns with the graphical illustration in Figure 1, capturing the idea that the social planner of a region can choose the level of carbon tax such that the firm can internalize the regional SCC and achieve its net emissions level of E^* , rather than E^m . When $E^* = 0$, the Karush-Kuhn-Tucker conditions of (17) shows that

$$\tau \geq \text{MAC}(E^*) - m. \quad (19)$$

That is, the carbon tax could be larger than the gap between the MAC of a region and the market price of emission permits. In particular, the regional $\text{MAC}(E^*)$ at $E^* = 0$ could be smaller than the global permit price m , in which case the optimal carbon tax should be zero. Since the optimal carbon tax can always be chosen to be equal to the gap between the MAC and the permit price when the gap is positive, we have the following general formula for any $E^* \geq 0$:

$$\tau = \max\{0, \text{MAC}(E^*) - m\}. \quad (20)$$

The simple relationship between the optimal carbon tax, the MAC, and the permit price is also verified in our numerical solutions of the dynamic regional model. Therefore, when we compare the regional SCC to the regional optimal carbon tax in our numerical results, we will compare it to the gap of the regional MAC and the permit price.

5 Data and Calibration

To calibrate our model with data, we have two objectives. The first objective is to generate regional emission cap pathways ($\overline{E}_{i,t}$) for future periods, constraining the constituent nations of each region to meet their commitments to the Paris Agreement and the net zero emission targets. The second objective is to determine parameters for total factor productivity ($A_{i,t}$), carbon intensity ($\sigma_{i,t}$), abatement cost ($b_{1,i}$, $b_{2,i}$, $b_{3,i}$), and climate damage ($\pi_{1,i}$, $\pi_{2,i}$) that reflect the future projections provided in recent studies (Burke et al., 2018;

Ueckerdt et al., 2019; Kahn et al., 2021). We obtain these region-specific parameters, which capture regional heterogeneities in GDP growth, emissions, technologies, and climate damages.

Our model’s 12 regions are formed by aggregating 198 countries around the world, following the regional classification in the RICE model (Nordhaus and Yang, 1996; Nordhaus, 2010). For the initial year 2020, we obtain country-level historical data on population (billions), capital (\$ trillions, 2020), GDP (\$ trillions, 2020), and emissions (GtC) from the World Bank. For future projections on population growth, we use the SSP2 scenario (Samir and Lutz, 2017).

5.1 Regional Emission Cap Pathways

Since there is no global cap-and-trade or ETS currently in place, we use the emission commitments of the Paris Agreement and the regions’ net zero commitments to construct the baseline emission cap constraint, $\bar{E}_{i,t}$. We collect reports of the Intended Nationally Determined Contributions (INDCs) of 165 countries that were submitted at the United Nations Framework Convention on Climate Change (UNFCCC) Conference of the Parties (COP 21) in Paris in December 2015 (INDC, 2023). Although there is no international enforcement mechanism, most countries committed to achieving a self-defined mitigation target for 2030 (or 2025). We also obtain the target years to reach net zero emissions of different countries from Climate Action Tracker (2023). Based on these datasets, we create the baseline regional emission cap pathways for future periods following the strategy detailed below.

As the first step, we obtain the level of emission targets by 2030 for each country. In their INDC reports, most countries expressed targets as a specific percentage reduction in emissions by 2030 (or, in some cases, 2025) compared to their Business As Usual (BAU) emission level in 2015. Some countries, including China, Chile, Malaysia, Singapore, and Tunisia specified their targets as a percentage reduction in carbon intensity instead of a percentage reduction in net emissions. For the countries that did not make a specific emissions reduction pledge, we assume that their carbon intensity reduction and emission

reduction percentages are the same as those of the most populous country in that region.

Next, we generate annual emission cap pathways based on the regions' historical emission levels (World Bank, 2020), their emission targets for 2030 (or 2025), and net zero emission target years. We use five-year emissions data (2014 - 2018) from the World Bank and the INDC emission targets in 2030 (or 2025) to fit a quadratic function and use this fitted function to project the emission pathways for the periods between 2018 and 2030. Emission projections for the years between 2030 (or 2025) and the net zero emission target year are obtained by linearly interpolating the emissions. After obtaining the country-level emission pathways, we aggregate them to find the regional emission cap pathways.⁶ To assess the implications of varying stringency in the emission caps, we also create additional emission cap pathways by choosing alternative net zero scenarios, wherein we assume that all regions achieve net zero emissions by 2050 (most stringent), 2070, or 2090 (most lax). See Figures A.2 and A.3 in Appendix A.4 for the regional emission cap pathways in the baseline cap scenario and the different emission cap pathways at the global level.

5.2 Total Factor Productivity

We calibrate total factor productivity (TFP), $A_{i,t}$, for future periods based on the GDP projections in Burke et al. (2018), who provide the projected GDP of 165 countries until 2099 assuming no climate-related impacts. We aggregate these projections according to our 12 regions and employ the SSP2 population scenario to obtain regional GDP per capita estimates, $y_{i,t}^{\text{BDD}}$, which are used to calibrate the regional TFP under no climate impacts, $A_{i,t}$. For each region i , the dynamic path of the TFP is modeled by the relationship $A_{i,t+1} = A_{i,t} \exp(g_{i,t})$, where $g_{i,t}$ is the growth rate of $A_{i,t}$ at time t . When

⁶We also find that our aggregated regional emission cap pathways are close to those used in Nordhaus (2010).

$t < 80$ (i.e., within this century), we assume

$$g_{i,t} = g_{i,0} \exp(-d_i t). \quad (21)$$

For $t \geq 80$ (i.e., beyond this century), since the cumulative effect is huge for a long horizon, it is often inappropriate to simply extrapolate TFP growth rate using the formula (21). Therefore, we follow RICE to generate $g_{t,i}$ for $t \geq 80$. See Appendix A.5 for the details.

In our structural estimation, we obtain $(g_{i,0}, d_i)$ by solving the following minimization problem:

$$\min_{g_{i,0}, d_i} \sum_{t=0}^{79} w_t \left(\frac{y_{i,t}^{\text{NoCC}}}{y_{i,0}^{\text{NoCC}}} - \frac{y_{i,t}^{\text{BDD}}}{y_{i,0}^{\text{BDD}}} \right)^2, \quad (22)$$

where w_t are weights, and $y_{i,t}^{\text{NoCC}}$ is GDP per capita obtained by solving the following optimal growth model with a choice of $(g_{i,0}, d_i)$ and its associated TFP A_{it} :

$$\begin{aligned} \max_{c_{i,t}} \quad & \sum_{t=0}^{500} \beta^t u(c_{i,t}) L_{i,t}, \\ \text{s.t.} \quad & K_{i,t+1} = (1 - \delta) K_{i,t} + (y_{i,t}^{\text{NoCC}} - c_{i,t}) L_{i,t}, \end{aligned} \quad (23)$$

where $y_{i,t}^{\text{NoCC}} = A_{i,t} K_{i,t}^\alpha L_{i,t}^{1-\alpha}$ is the GDP per capita under no climate impact and $u(c_{i,t})$ is defined as in equation (7). The initial TFP $A_{i,0}$ is chosen such that $A_{i,0} K_{i,0}^\alpha L_{i,0}^{1-\alpha}$ is equal to the observed GDP per capita in 2020. Figure A.4 in Appendix A.6 shows that with our calibrated $A_{i,t}$, the GDP per capita $y_{i,t}^{\text{NoCC}}$ matches well with the projected data $y_{i,t}^{\text{BDD}}$ from Burke et al. (2018) for all regions.

5.3 Carbon Intensity

To obtain the time-varying and region-specific carbon intensities $\sigma_{i,t}$, we use the projections of GDP and emissions in Ueckerdt et al. (2019), who report simulation results of future emissions and GDP under different scenarios based

on climate policy regimes, technology portfolios, and carbon tax implementation. As the carbon intensity in our model reflects the zero-carbon tax regime, we employ results from the scenario defined as ‘FFrun211’ in Ueckerdt et al. (2019). Specifically, this FFRun211 scenario corresponds to climate action from 2020 with full technology portfolio but with zero carbon tax. Based on the equation (1), we calculate the carbon intensities as $\sigma_{i,t} = E_{i,t,\text{FFrun211}}^U / Q_{i,t,\text{FFrun211}}$, where $E_{i,t,\text{FFrun211}}^U$ and $Q_{i,t,\text{FFrun211}}$ are the projected regional emissions and GDP under the FFRun211 scenario for region i at time t .⁷

5.4 Abatement Cost

Our estimation of the abatement cost parameters $b_{1,i}$, $b_{2,i}$, and $b_{3,i}$ relies on the simulation results under ten different levels of carbon taxes in Ueckerdt et al. (2019). For each scenario j with associated carbon taxes $\tau_{t,j}^U$, Ueckerdt et al. (2019) report the projected regional emissions net of abatement ($E_{i,t,j}^U$), for region i at time t . Since Ueckerdt et al. (2019) do not consider an ETS, according to the discussion in Section 4.2, we can assume that their carbon taxes $\tau_{t,j}^U$ are equal to the marginal abatement costs when net emissions are strictly positive. That is,

$$\tau_{t,j}^U = \frac{1,000 b_{2,i} \mu_{i,t,j}^{b_{2,i}-1} b_{1,i,t}}{\sigma_{i,t}} = 1,000 b_{2,i} \mu_{i,t,j}^{b_{2,i}-1} (b_{1,i} + b_{3,i} \exp(-b_{4,i}t)), \quad (24)$$

for $\mu_{i,t,j} \in (0, 1)$. Therefore, we can use their simulation results under different carbon tax levels to estimate $b_{1,i}$, $b_{2,i}$, $b_{3,i}$, and $b_{4,i}$. At first, we estimate the associated emission control rate $\mu_{i,t,j}^U$ using the equations (1)-(3) as follows:

$$\mu_{i,t,j}^U = 1 - \frac{E_{i,t,j}^U}{E_{i,t,\text{FFrun211}}^U}, \quad (25)$$

⁷Ueckerdt et al. (2019) provide data for 11 regions. Upon comparison, we find that the countries constituting the ‘Rest of the World (ROW)’ region are the ones that are in the ‘Other High Income (OHI)’ and ‘Eurasia’ region in our study. Therefore, the carbon intensity obtained from the ROW in Ueckerdt et al. (2019) corresponds to that of OHI and Eurasia regions in our work.

where $E_{i,t,\text{FFrun211}}^U$ is the regional emissions from the FFFrun211 scenario with zero carbon tax (see Ueckerdt et al. (2019) for details). Then we use the computed $\mu_{i,t,j}^U$ and the associated carbon tax $\tau_{t,j}^U$ to find the abatement cost coefficients— $b_{1,i}$, $b_{2,i}$, $b_{3,i}$, and $b_{4,i}$ —such that the equality (24) can hold in an approximate manner for every scenario j and time t .

5.5 Climate Damage

We calibrate the climate damage parameters $\pi_{1,i}$ and $\pi_{2,i}$ by considering projections on GDP loss across different climate scenarios in Kahn et al. (2021), which shows the percentage loss in GDP per capita by 2030, 2050, and 2100 under the RCP 2.6 and RCP 8.5 scenarios for China, EU, India, Russia, and the US. We use their method and data to project the percentage loss in GDP per capita ($\Delta_{i,t}^{\text{RCP26}}$ and $\Delta_{i,t}^{\text{RCP85}}$) every year from 2020 to 2114 under the RCP 2.6 and RCP 8.5 scenarios for each of our 12 regions, employing the baseline setup in Kahn et al. (2021). Specifically, $\Delta_{i,t}^{\text{RCP26}} = 1 - y_{i,t}^{\text{RCP26}}/y_{i,t}^{\text{base}}$ and $\Delta_{i,t}^{\text{RCP85}} = 1 - y_{i,t}^{\text{RCP85}}/y_{i,t}^{\text{base}}$, where $y_{i,t}^{\text{RCP26}}$, $y_{i,t}^{\text{RCP85}}$, and $y_{i,t}^{\text{base}}$ are GDP per capita under RCP 2.6, RCP 8.5, and the baseline scenario, respectively. Thus from equation (9) we obtain $(\pi_{1,i}, \pi_{2,i})$ by solving the following minimization problem for each region i :

$$\min_{\pi_{1,i}, \pi_{2,i}} \sum_{t=0}^{94} \left(\frac{1 + \pi_{1,i} T_t^{\text{RCP85}} + \pi_{2,i} (T_t^{\text{RCP85}})^2}{1 + \pi_{1,i} T_t^{\text{RCP26}} + \pi_{2,i} (T_t^{\text{RCP26}})^2} - \frac{1 - \Delta_{t,i}^{\text{RCP26}}}{1 - \Delta_{t,i}^{\text{RCP85}}} \right)^2. \quad (26)$$

Here T_t^{RCP26} and T_t^{RCP85} are the global average temperature anomalies at time t (deviation from the pre-industrial temperature) under the RCP 2.6 and RCP 8.5 scenarios. Figure A.5 in Appendix A.7 shows that with our calibrated climate damage coefficients, the ratios of GDP per capita between RCP 2.6 and RCP8.5 from our model, matches well with the ratios in Kahn et al. (2021), for every region.

6 Results

In this section, we discuss our simulation results. We first present the results of the noncooperative model under the baseline emission cap scenario for 2020 to 2100. Next, we compare the economic outcomes of different models: noncooperation versus cooperation, with or without the emission caps, and with or without the global ETS. Lastly, we present simulation results with the different emission cap scenarios assuming the net zero target year to be 2050, 2070, and 2090, respectively, for all countries.

6.1 Noncooperation with ETS under the Baseline Emission Caps

Figure 2 displays simulation results at the global level, from the noncooperative model with the ETS under the baseline emission cap scenario. Until 2100, we can delineate three periods according to the global emission trading patterns. Prior to 2032, global emissions do not reach the global emission cap and therefore the permit price remains zero, implying an excess supply of emission permits in the first decade (Figure 2 top-left and bottom-left). This result is not surprising, considering that an oversupply of emission permits has been observed in the EU ETS (Fuss et al., 2018), resulting in zero or very low permit prices. During this period, the volume of global emission abatement and its associated abatement cost remain at low levels (Figure 2 top-left and bottom-right). This result implies that the global emission cap should be set at a level such that there is no over-supply of emission permits, so that permit prices are strictly positive under noncooperation and the ETS.

Global emissions are constrained by the global emission caps starting from 2032. To comply with the monotonically decreasing emission caps, the regions undertake additional abatement efforts and/or purchase emission permits. This results in a substantial increase in the volumes of both emission abatement and traded permits, along with their associated costs. The decrease in global emissions is mainly achieved by the concomitant increase in global abatement, which peaks by around 2065 (Figure 2 top-left). The global abate-

ment cost also increases steeply to reach its maximum value of \$5.2 trillion by 2070, and then decreases as the world reaches net zero emissions by 2070. The emission permit trade, which rises from 2020, gradually decreases to zero by 2070 (Figure 2 top-left). As the emission cap becomes tighter over the years, the permit price increases to \$749 per ton of carbon in 2050 and \$2,225 in 2069 (Figure 2 bottom-left). The kinks in the permit price path in 2050 and 2060 are a result of some regions achieving net zero emissions. As shown in Figure A.2, under the baseline emission cap scenario, the net zero target year is 2050 for the US, EU, Japan, and OHI regions, and 2060 for Russia and China. Essentially, binding emission caps lead to a rise in the overall emission abatement, while the steep increase in the permit price limits the trading of emission permits.

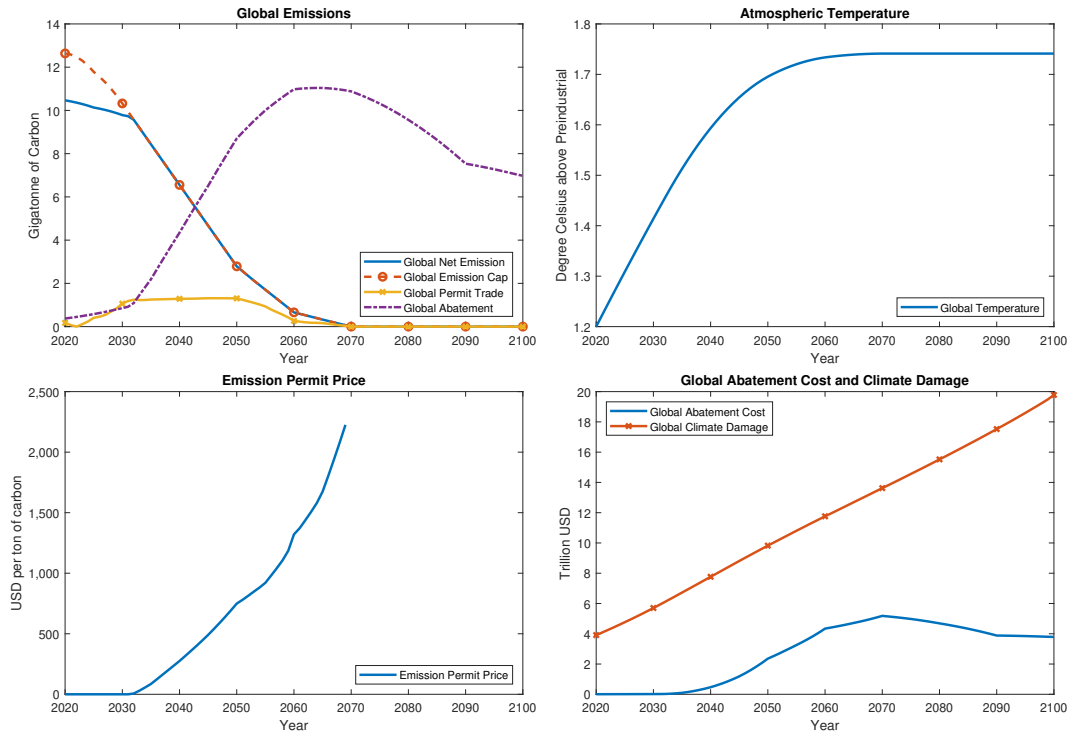


Figure 2: Simulation results at the global scale for the noncooperative model with emission trading under the baseline emission cap scenario.

Post-2070 is the period when global emissions are net zero. For this period,

emission permits are no longer traded and all emissions are abated in each region.⁸ By the end of this century, the atmospheric temperature is projected to reach 1.74 degrees Celsius above the pre-industrial level, which is driven by net positive emissions before 2070 (Figure 2 top-right). Lastly, the global climate damage costs rise almost linearly over the entire period (Figure 2 bottom-right). Overall, our noncooperative model simulation predicts that the global emission caps set by the Paris Agreement are not restrictive enough to achieve the global target of limiting the temperature rise to 1.5 degrees Celsius.

It is instructive to examine the trading patterns of different regions in the emission permit market over the years to identify the permit buyers and sellers. Figure 3 displays the volumes of traded emission permits for each region over time, with a positive value denoting permit purchase and a negative value indicating permit sales. In the first decade, although there is an excess permit supply at the global level, the emission cap constraint is effective for some regions, such as the United States and Latin America, as these regions become permit buyers at this early stage. After 2032, when the global emission cap constraint becomes binding, the group of permit buyers expands to the US, EU, India, Middle East, Africa, and OHI regions, with the US and India being the largest permit buyers. The group of permit sellers consists of Russia, China, Eurasia, OthAs, and Latin America, with China being the largest permit provider. Japan is expected to be involved in a relatively small volume of permit trading.

Based on our simulation results, we now discuss the optimal regional carbon tax under the noncooperative model with the ETS and the baseline emission cap scenario. Figure 4 shows the regional MAC along with the market equilibrium price of emission permits. We find that the MAC of every region increases drastically and remains strictly greater than the permit price until 2050, and the net emissions are strictly positive for all regions during this time.

⁸In the bottom-left panel of Figure 2, we plot the emission permit price only when the traded volume is positive.

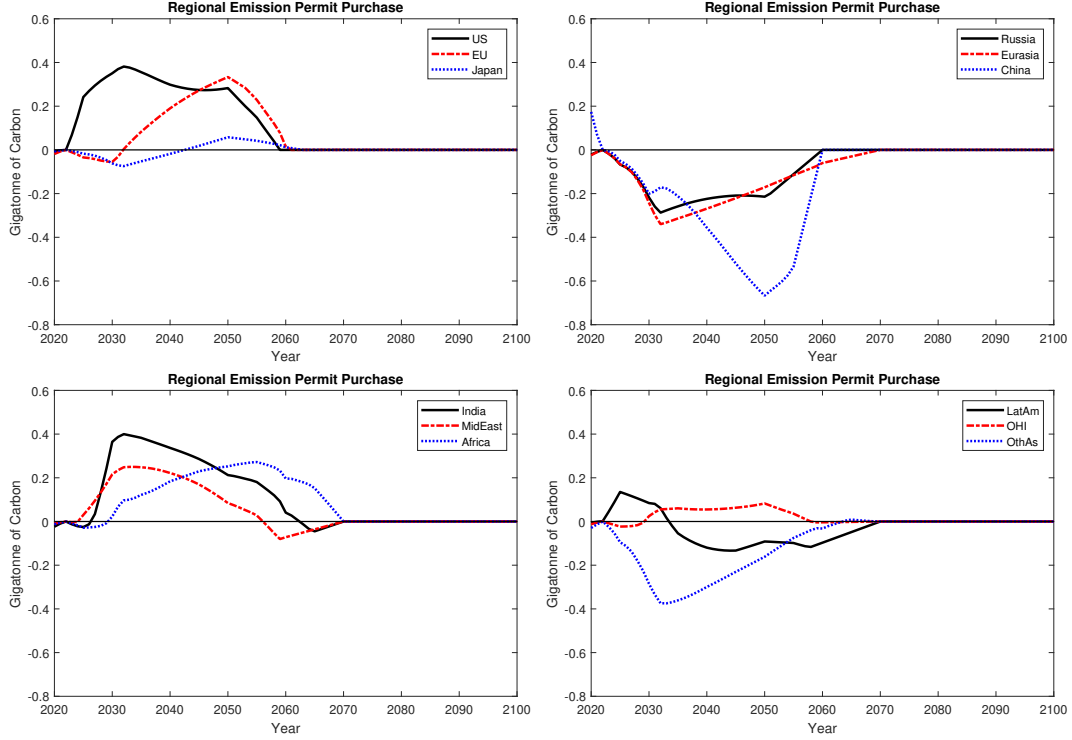


Figure 3: Simulation results of regional emission permit purchase for the non-cooperative model with emission trading, under the baseline emission cap scenario.

⁹ As discussed in Section 4.2, $\text{MAC}(E_{i,t}^*) > m_t$ is equivalent to $E_{i,t}^* < E_{i,t}^m$, implying that when there is no carbon tax, the optimal net emissions for the social planner do not align with the optimal net emissions for the representative firm in each region. Therefore, the optimal carbon tax can be determined by $\tau_{i,t} = \text{MAC}(E_{i,t}^*) - m_t$, so that the firm's net emissions are equal to the social planner's optimal net emissions $E_{i,t}^*$, for region i at time t before 2050.

In Figure 4, the MAC of each region gradually decreases below the permit price after its net zero emissions (before trading of permits) is achieved. Russia is the first region to achieve net zero emissions (before trading of permits) in 2051 (as shown in Figure A.6 in Appendix A.8.1). But Russia still sells permits afterwards, as shown in Figure 3, because its after-trade net zero emission

⁹For regional optimal net emissions, see Figure 3 in Appendix A.8.1.

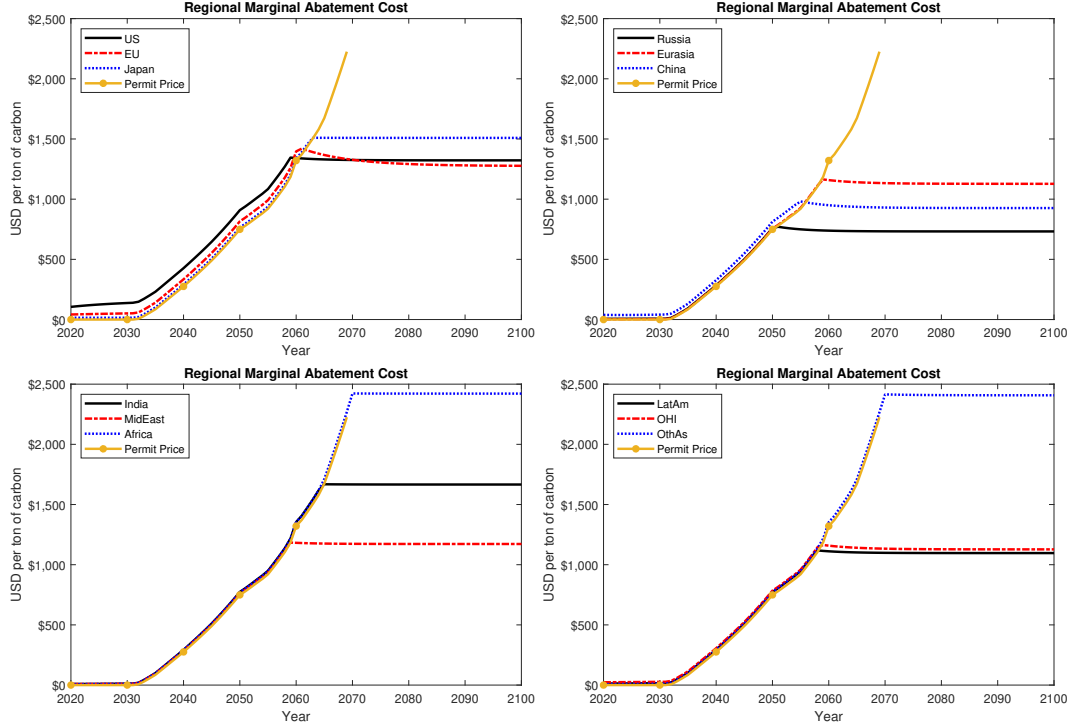


Figure 4: Simulation results of regional MAC for the noncooperative model with emission trading under the baseline emission cap scenario.

target year is 2060 under the baseline emission cap scenario. After 2051, Russia's MAC declines below the permit price, because its emission control rate has reached its upper bound. Similar trends are followed by other regions as they attain zero net emissions (before trading of permits) in the 2050s (China and Eurasia) and the 2060s (the US, the EU, Japan, MidEast, Latin America, and the OHI). India, Africa, and non-OECD Asia are the last group of regions to achieve net zero emissions (before trading of permits) by 2070, after which emission permits are no longer traded, and the MACs of all regions decline slowly over time.¹⁰ Recall that, when the regional net zero emissions (before trading of permits) are achieved, the optimal carbon tax should be larger than the gap between MAC and permit price, i.e., $\tau_{i,t} \geq \text{MAC}(E_{i,t}^*) - m_t$. Note that if a region's after-permit-trade zero emission cap constraint is binding, then

¹⁰When emission control rates are one, the MACs are $1,000b_{2,i}(b_{1,i} + b_{3,i} \exp(-b_{4,i}t))$, and they are nearly constant when t is large.

even when its regional MAC is smaller than the permit price, the region will not be able to sell emission permits, otherwise it will violate the constraint.

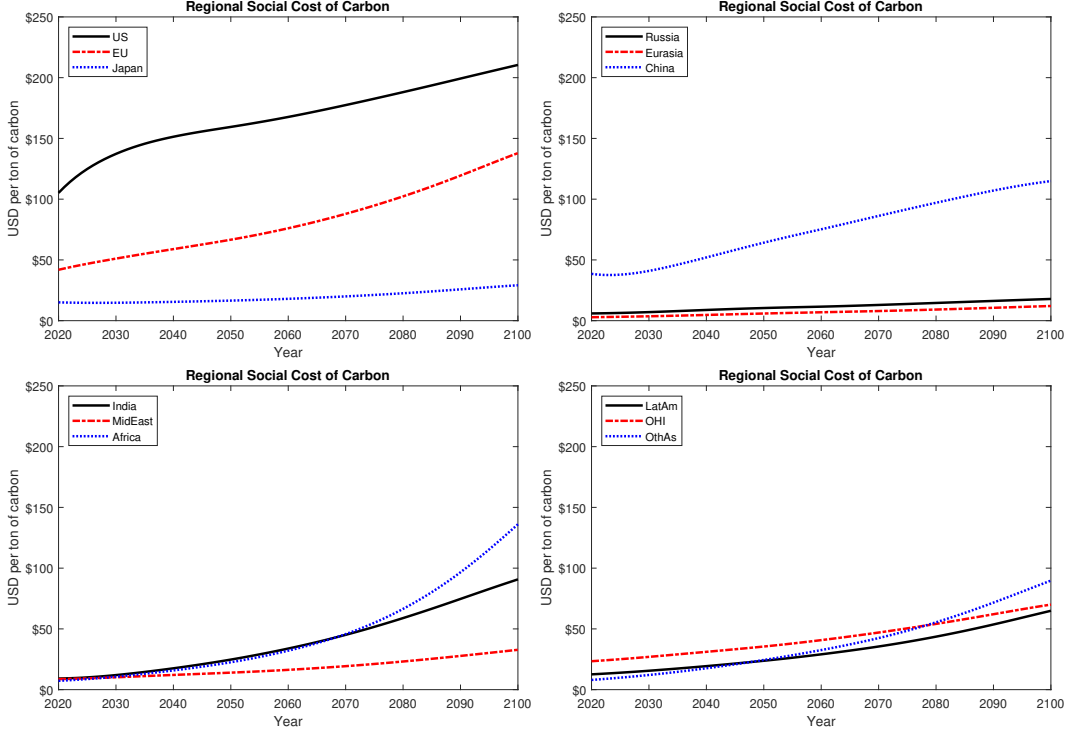


Figure 5: Simulation results of regional SCC for the noncooperative model with emission trading under the baseline emission cap scenario.

We further confirm the relationship between the optimal regional carbon tax and the regional SCC under noncooperation with the ETS. Figure 5 shows that when the net emissions of a region are strictly positive, the regional SCC is exactly equal to the optimal carbon tax, which is equal to the gap between the regional MAC and the permit price in Figure 4. For example, in 2050, the MAC for the US is \$908 per ton of carbon, the permit price is \$749, and their difference is exactly equal to the regional SCC of the US, \$159. Figure 5 also shows that when the regional net emissions is zero, the regional SCC is larger than the gap, which could be negative. Among all the regions, the US has the highest SCC, starting at \$105 per ton of carbon in 2020 and steadily increasing up to \$210 per ton of carbon by the end of this century. The US is

followed by the EU (from \$42 to \$138 per ton of carbon) and China (from \$39 to \$115 per ton of carbon) in this century. The regions with the lowest SCC in 2100 are Japan (\$29 per ton of carbon), Russia (\$18 per ton of carbon), Eurasia (\$12 per ton of carbon), and MidEast (\$33 per ton of carbon). Our results show that there is considerable heterogeneity in the SCC across regions and suggest that a significant amount of regional carbon tax implementation is required, particularly for the US, the EU, and China, under the global ETS with the baseline emission cap scenario.

6.2 Comparative Analysis of Different Cases

We now modify our baseline model with various cases to understand the implications of cooperation among regions and the ETS. We compare outcomes between the noncooperative and the cooperative models, and for each model, we examine the impact of the ETS under the baseline emission caps. Figure 6 displays the global emission and temperature time profiles for all the cases. Note that for the cooperative model with the ETS, we use the equilibrium solution of permit prices obtained under the noncooperative model with the ETS, so we can compare the difference in the solutions between cooperation and noncooperation, holding permit prices fixed across scenarios.

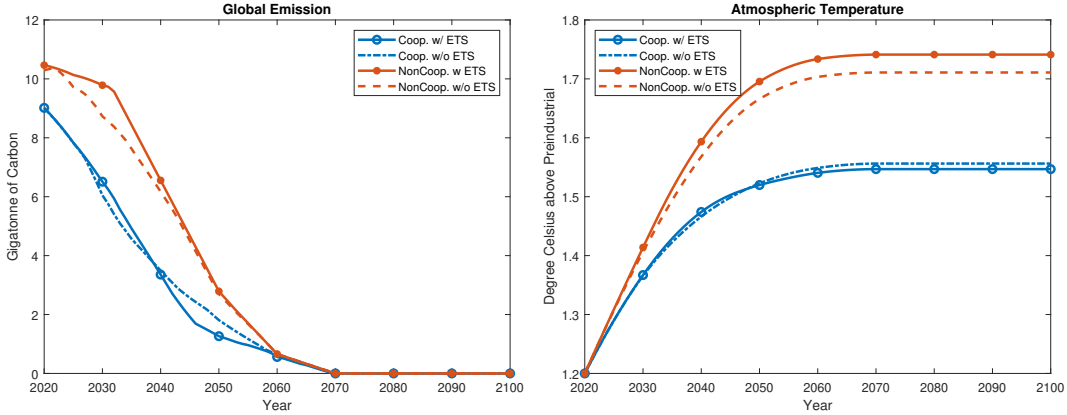


Figure 6: Simulation results of different cases under cooperation or noncooperation.

We observe that under cooperation, with the objective of maximizing the

sum of discounted utility of all the regions, emissions and temperature rises are lower than their counterparts under noncooperation. Specifically, cooperation results in approximately 0.19 degrees Celsius lower temperature with the ETS and 0.15 degrees Celsius lower temperature without the ETS. Our findings underscore that global cooperation is still helpful in mitigating climate change even when every region has the baseline emission caps.

When comparing the cases with and without the ETS, we find that the ETS may play different roles under noncooperation and cooperation. In the noncooperative model, implementation of the ETS results in slightly higher emissions and temperature rises compared to the case without the ETS. This is because with the ETS, regions with binding regional emission cap constraints now have the option to purchase permits from regions with less restrictive emission caps, fully exploiting the total amount of permits allowed at the global level. This happens until 2050. In the cooperative model, on the other hand, the impact of the ETS on global emissions and temperature changes over time. With the ETS, slightly higher levels of global emissions and temperature rise are observed before 2040 and 2050, respectively, and the opposite trends are observed after that. This evolving pattern suggests that the ETS serves as a channel to redistribute emissions, such that the sum of discounted utility of all regions can be maximized over time.

We also compare the regional MAC and SCC across the different cases. Figure 7 presents the regional MAC and SCC under both the cooperative and the noncooperative models with or without the ETS, using the US as an illustrative example.¹¹ Under cooperation, the MAC of the US (Figure 7 top-left) is very large in the initial years. This is because the US, as a developed region, needs to mitigate a significant amount of emissions so that developing regions can mitigate less (as shown in Figure A.9 in Appendix A.8.3), thus improving global social welfare. After the 2030s, however, the US net emissions become zero in the cooperative case¹² and cannot be further mitigated, so its MAC starts to decline over time. The effect of the ETS

¹¹For comparisons of other regions, refer to Appendices A.8.4 and A.8.3.

¹²For regional net emissions under cooperation and noncooperation, see Appendix A.8.2.

depends on the magnitude of the MAC (see Figure A.9 in Appendix A.8.3): if a region is developed but its MAC is high, then in the ETS, the region would abate less as it can purchase permits (e.g., the US); if a region is developed but its MAC is not too high, then in the ETS, it would abate more (and buy permits at the same time) to improve global social welfare (e.g., the EU at around 2040); if a region is developing but has small MAC and loose cap constraints, then in the ETS, it would abate more so the region can sell permits with a higher return (e.g., LatAm).

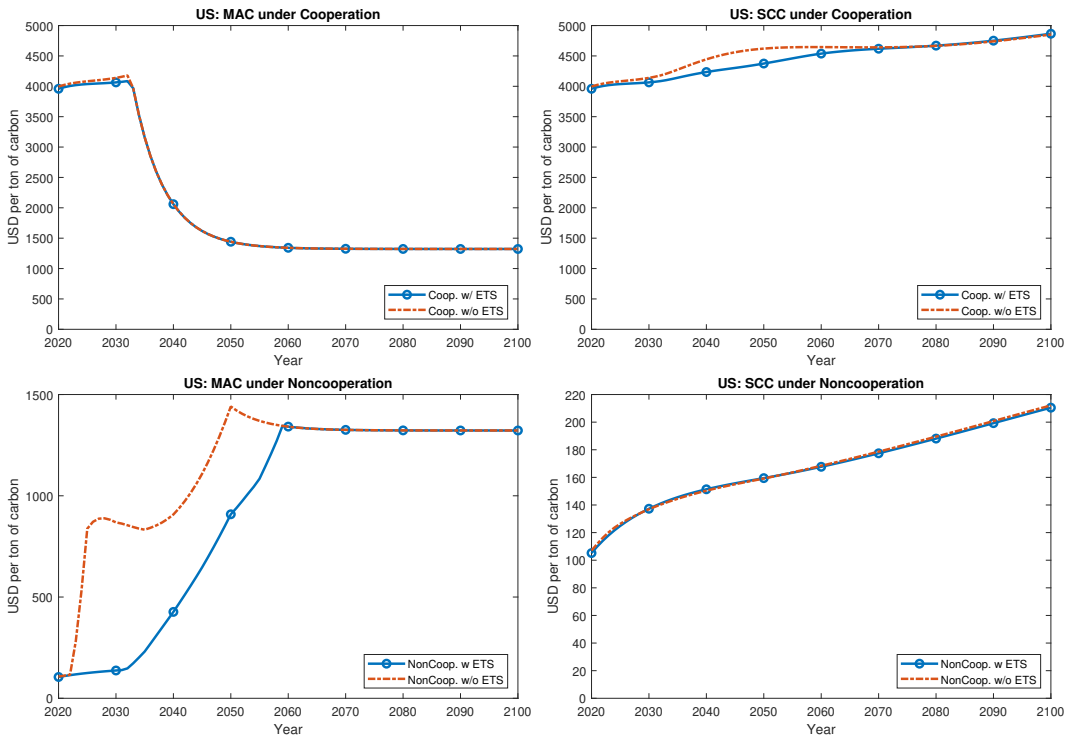


Figure 7: Simulation results of different cases for the US in the cooperative or noncooperative model.

The top-right panel of Figure 7 shows that the cooperative SCC of the US is sustained at a high level throughout all periods. This is consistent with the high MAC of the US. When the US regional net emissions are not binding at zero before 2032, the regional SCC is equivalent to the optimal regional carbon tax, which is also equal to the regional MAC, as the exoge-

nous permit price (from the noncooperative model's solution) is zero before 2032. Moreover, from our definition of cooperative SCC, we can see that a developed region will have a high SCC, as the marginal global welfare over capital, $\partial V_t^{\text{Coop}}/\partial K_{i,t}$, for the developed region is relatively small, while the marginal global welfare over emissions, $\partial V_t^{\text{Coop}}/\partial \mathcal{E}_t$, is the same across regions. This also implies that a developed region will contribute more to mitigating emissions under cooperation. This pattern is consistent across regions: Figure A.11 in Appendix A.8.4 shows that the US, EU, Japan and OHI have a high cooperative SCC, while the developing regions like India and Africa have a small cooperative SCC.

Under noncooperation, the MAC of the US is substantially lower in the case with the ETS compared to the case without the ETS (Figure 7, bottom-left panel). Such discrepancy persists until 2058, the period during which the US is a net permit buyer (shown in Figure 3), reflecting the fact that implementation of the ETS offers the US a more cost-effective means of keeping its net emissions below its cap. Consequently, the US conducts less emission abatement. For all other regions, we find that the MAC is consistently lower (higher) with the ETS compared to the case without the ETS when a region is a buyer (seller) across all periods with nonzero permit prices from 2032 (see Figure A.10 in Appendix A.8.3).

The bottom-right panel of Figure 7 shows that the noncooperative SCC of the US is much smaller than its cooperative SCC, which is also consistent with the smaller MAC of the US under noncooperation. Moreover, every region has a much smaller SCC under noncooperation than under cooperation, as shown in Figures A.11 and A.12 in Appendix A.8.4. This result implies that, in the dynamic Nash equilibrium under noncooperation, no region is willing to impose a high carbon tax thereby allowing other regions to free ride on lower emissions and climate damages. Therefore, in the noncooperative model, emissions and temperature rises are much larger than in the cooperative model, as shown in Figure 6.

Now we confirm the relationship between the optimal regional carbon tax and the regional SCC when there is no ETS. For the cooperative case without

the ETS, the US regional net emissions are not binding at their caps, but are binding at zero after 2032 (see Figure A.7), so the regional SCC is larger than the regional MAC after 2032 (see the two top panels of Figure 7), which is equal to the optimal regional carbon tax under cooperation. For the noncooperative case without the ETS, the US regional net emissions are binding at their caps (see Figures A.2 and A.8), so the regional SCC is smaller than the regional MAC (see the two bottom panels of Figure 7), which is equal to the optimal regional carbon tax under noncooperation. Moreover, under no ETS, if the regional net emissions are not binding at their caps or zero, then the regional SCC is equal to the regional MAC (see, e.g., Russian under cooperation until 2057 in Figures A.7, A.9, A.11); and Russian under noncooperation until 2042 in Figures A.8, A.10, and A.12). This relationship holds for every region as shown in Figures A.7-A.12.

The two right panels of Figure 7 collectively demonstrate that the ETS has relatively little impact on the regional SCC under both cooperation and noncooperation. This pattern holds for every region as shown in Figures A.11 and A.12.

6.3 Alternative Net Zero Scenarios

Along with the baseline emission cap scenario, we further analyze simulation results for the noncooperative model with alternative emission cap paths, defined by the net zero emission targets in 2050, 2070, and 2090. The top-left and top-right panels in Figure 8 display the emission permit prices and expected temperature increases under different emission cap scenarios. Under the net zero 2050 scenario, which is the most strict emission cap schedule, the emission permit price reaches \$1,538 per ton of carbon in 2049, and the temperature rise is restricted to 1.64 degrees Celsius by the end of this century. Net zero 2070 and net zero 2090 are more relaxed scenarios, leading to permit prices at \$344 and \$158 per ton of carbon in 2049, respectively. In these scenarios, the temperature rise by the end of the century is expected to reach 1.86 degrees Celsius and 2.08 degrees Celsius above the pre-industrial level, respectively.

This result shows that the global target of restricting the temperature rise to 1.5 degrees Celsius is unattainable in a noncooperative world, even under the most restrictive net zero 2050 scenario, suggesting that stronger measures are needed to effectively regulate global emissions.

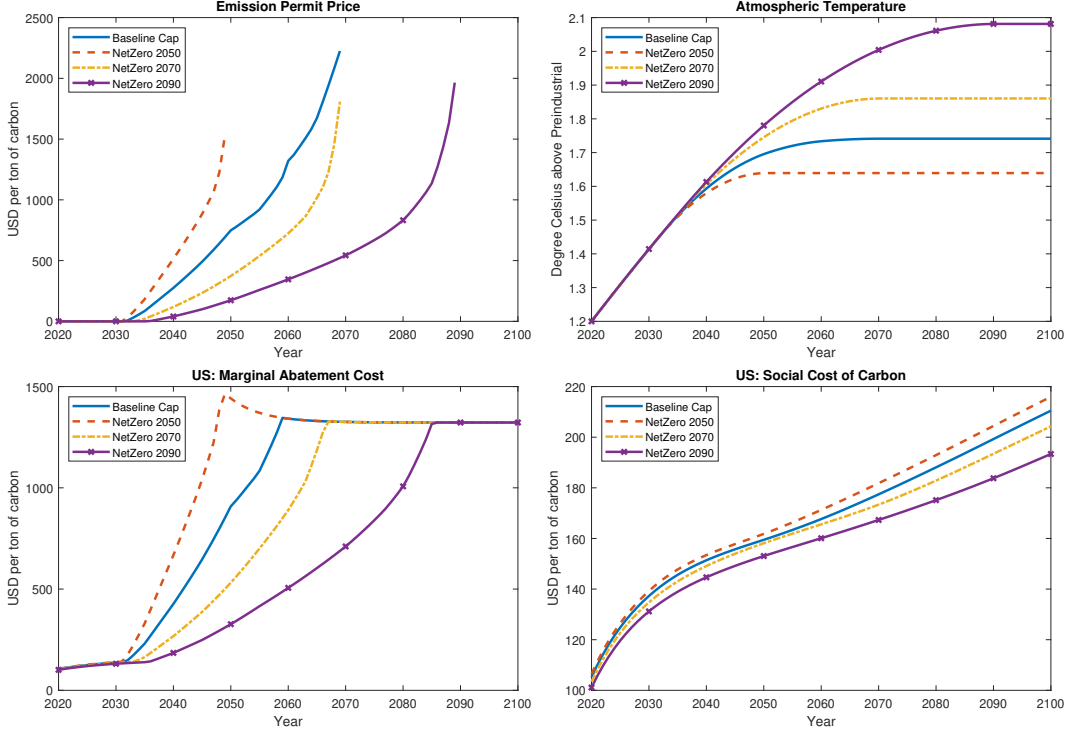


Figure 8: Simulation results of alternative emission cap scenarios under non-cooperation with the ETS.

The bottom-left and bottom-right panels in Figure 8 show the regional MAC and SCC, taking the US as an example. The comparison of the regional SCC and MAC for all other regions are available in Appendix A.8.5, which show the same patterns as the US. Our results show that stricter emission caps lead to higher MACs. Specifically, the MAC of the US under the net zero 2050 scenario can reach up to \$1,465 per ton of carbon in 2049, compared to the peak of \$1,323 in 2086 under the net zero 2090 scenario. This is because more rigorous emission caps imposed on each region entail additional abatement efforts, resulting in a higher MAC. We also find that more stringent emission

caps result in a smaller SCC: the SCC of the US is \$216 per ton of carbon in 2100 in the net zero 2050 scenario, while it is \$193 in 2100 in the net zero 2090 scenario. This is because the permit price grows more quickly over time and even faster than the MAC (note that the optimal carbon tax is equal to the gap between the MAC and permit price when net emissions are strictly positive). Our finding suggests that under a stricter regulation on emission caps, carbon taxation becomes a less important policy instrument to control emissions.

7 Conclusion

In this work, we build a dynamic multi-region model of climate and the economy with a global emission cap-and-trade system. In our integrated assessment framework, 12 aggregated regions are allocated emission caps in line with the emission targets of the Paris Agreement and their net zero commitments. We solve for the market prices of emission permits under the dynamic Nash equilibrium in a noncooperative setting. The permit prices are endogenously determined by demand and supply of emission permits in the global permits market, reflecting regional heterogeneity in future productivity growth, abatement technologies, climate damage, and population growth. We further show that carbon taxation can be introduced under the global ETS as a complementary policy to help the social planner of each region achieve their optimal net emissions. For strictly positive net emissions, we have shown both theoretically and numerically that the optimal carbon tax is equal to the difference between the regional MAC and the market price of permits.

This work has several policy implications. First, our results indicate that the current global target of restricting the global temperature rise to 1.5 degrees Celsius above pre-industrial levels by 2100 is unattainable under noncooperation, even with the current emission commitments outlined in the Paris Agreement. Our findings suggest that more stringent emission reduction targets and global cooperation are needed to curb the trend of rising global temperature. Second, our baseline simulation shows that the current emission

commitments of the Paris Agreement lead to excess emission permit supply in the initial decade, resulting in permit prices of zero. This finding suggests that effective implementation of the global ETS requires stricter emission caps so that the global supply of permits does not exceed the global demand of permits. Third, we demonstrate that the global ETS is not a pure substitute for the carbon tax, but instead that both can be implemented together to improve the efficiency of global climate policies.

References

- Paola Arias, Nicolas Bellouin, Erika Coppola, Richard Jones, Gerhard Krinner, Jochem Marotzke, Vaishali Naik, Matthew Palmer, G-K Plattner, Joeri Rogelj, et al. Climate change 2021: The physical science basis. contribution of working group i to the sixth assessment report of the intergovernmental panel on climate change; technical summary. 2021.
- Michael Barnett, William Brock, and Lars Peter Hansen. Pricing Uncertainty Induced by Climate Change. *The Review of Financial Studies*, 33(3):1024–1066, 2020.
- Severin Borenstein, James Bushnell, Frank A. Wolak, and Matthew Zaragoza-Watkins. Expecting the Unexpected: Emissions Uncertainty and Environmental Market Design. *American Economic Review*, 109(11):3953–3977, 2019.
- William Brock and Anastasios Xepapadeas. Climate change policy under polar amplification. *European Economic Review*, 99:93–112, 2017.
- Marshall Burke, W Matthew Davis, and Noah S Diffenbaugh. Large potential reduction in economic damages under un mitigation targets. *Nature*, 557(7706):549–553, 2018.
- Yongyang Cai and Thomas S Lontzek. The social cost of carbon with economic and climate risks. *Journal of Political Economy*, 127(6):2684–2734, 2019.

- Yongyang Cai, Kenneth L. Judd, and Thomas S. Lontzek. The social cost of carbon with economic and climate risks. Hoover economics working paper 18113, 2017. URL <https://www.hoover.org/research/social-cost-carbon-economic-and-climate-risk>.
- Yongyang Cai, William Brock, and Anastasios Xepapadeas. Climate change impact on economic growth: Regional climate policy under cooperation and noncooperation. *Journal of the Association of Environmental and Resource Economists*, 10(3):569–605, 2023.
- Jared C Carbone, Carsten Helm, and Thomas F Rutherford. The case for international emission trade in the absence of cooperative climate policy. *Journal of environmental economics and management*, 58(3):266–280, 2009.
- Climate Action Tracker, Apr 2023. URL <https://climateactiontracker.org/countries/>.
- Simon Dietz and Frank Venmans. Cumulative carbon emissions and economic policy: in search of general principles. *Journal of Environmental Economics and Management*, 96:108–129, 2019.
- Simon Dietz, Frederick van der Ploeg, Armon Rezai, and Frank Venmans. Are Economists Getting Climate Dynamics Right and Does It Matter? *Journal of the Association of Environmental and Resource Economists*, 8(5):895–921, 2021.
- Baran Doda, Simon Quemin, and Luca Taschini. Linking permit markets multilaterally. *Journal of Environmental Economics and Management*, 98:102259, 2019.
- Carolyn Fischer and Michael Springborn. Emissions targets and the real business cycle: Intensity targets versus caps or taxes. *Journal of Environmental Economics and Management*, 62(3):352–366, 2011.
- Meredith Fowlie, Mar Reguant, and Stephen P. Ryan. Market-based emissions

- regulation and industry dynamics. *Journal of Political Economy*, 124(1): 249–302, 2016.
- Sabine Fuss, Christian Flachsland, Nicolas Koch, Ulrike Kornek, Brigitte Knopf, and Ottmar Edenhofer. A framework for assessing the performance of cap-and-trade systems: insights from the european union emissions trading system. *Review of Environmental Economics and Policy*, 2018.
- Lawrence H Goulder and Andrew R Schein. Carbon taxes versus cap and trade: a critical review. *Climate Change Economics*, 4(03):1350010, 2013.
- Lawrence H Goulder, Marc AC Hafstead, and Michael Dworsky. Impacts of alternative emissions allowance allocation methods under a federal cap-and-trade program. *Journal of Environmental Economics and management*, 60(3):161–181, 2010.
- Lawrence H Goulder, Xianling Long, Jieyi Lu, and Richard D Morgenstern. China’s unconventional nationwide co2 emissions trading system: Cost-effectiveness and distributional impacts. *Journal of Environmental Economics and Management*, 111:102561, 2022.
- Wolfgang Habla and Ralph Winkler. Strategic delegation and international permit markets: Why linking may fail. *Journal of environmental economics and management*, 92:244–250, 2018.
- Christoph Hambel, Holger Kraft, and Eduardo Schwartz. The social cost of carbon in a non-cooperative world. *Journal of International Economics*, 131:103490, 2021.
- Steffen Hitzemann and Marliese Uhrig-Homburg. Equilibrium price dynamics of emission permits. *Journal of Financial and Quantitative Analysis*, 53(4): 1653–1678, 2018.
- Bjart Holtmark and Martin L Weitzman. On the effects of linking cap-and-trade systems for co 2 emissions. *Environmental and Resource Economics*, 75(3):615–630, 2020.

Katinka Holtsmark and Kristoffer Midttømme. The dynamics of linking permit markets. *Journal of Public Economics*, 198:104406, 2021.

INDC. Intended nationally determined contributions (indc), 2023. URL <https://www4.unfccc.int/sites/submissions/INDC/Submission%20Pages/submissions.aspx>

Niko Jaakkola and Frederick Van der Ploeg. Non-cooperative and cooperative climate policies with anticipated breakthrough technology. *Journal of Environmental Economics and Management*, 97:42–66, 2019.

Matthew E Kahn, Kamiar Mohaddes, Ryan NC Ng, M Hashem Pesaran, Mehdi Raissi, and Jui-Chung Yang. Long-term macroeconomic effects of climate change: A cross-country analysis. *Energy Economics*, 104:105624, 2021.

Linus Mattauch, H. Damon Matthews, Richard Millar, Armon Rezai, Susan Solomon, and Frank Venmans. Steering the Climate System: Using Inertia to Lower the Cost of Policy: Comment. *American Economic Review*, 110(4):1231–1237, 2020.

H. Damon Matthews, Nathan P. Gillett, Peter A. Stott, and Kirsten Zickfeld. The proportionality of global warming to cumulative carbon emissions. *Nature*, 459(7248):829–832, June 2009. ISSN 1476-4687. doi: 10.1038/nature08047.

Malte Meinshausen, Steven J Smith, Katherine Calvin, John S Daniel, Mikiko LT Kainuma, Jean-Francois Lamarque, Kazuhiko Matsumoto, Stephen A Montzka, Sarah CB Raper, Keywan Riahi, et al. The rcg greenhouse gas concentrations and their extensions from 1765 to 2300. *Climatic change*, 109:213–241, 2011.

William Nordhaus. *A question of balance: Weighing the options on global warming policies*. Yale University Press, 2014.

- William D Nordhaus. Economic aspects of global warming in a post-copenhagen environment. *Proceedings of the National Academy of Sciences*, 107(26):11721–11726, 2010.
- William D Nordhaus. Revisiting the social cost of carbon. *Proceedings of the National Academy of Sciences*, 114(7):1518–1523, 2017.
- William D Nordhaus and Zili Yang. A regional dynamic general-equilibrium model of alternative climate-change strategies. *The American Economic Review*, pages 741–765, 1996.
- Grischa Perino, Maximilian Willner, Simon Quemin, and Michael Pahle. The european union emissions trading system market stability reserve: does it stabilize or destabilize the market? *Review of Environmental Economics and Policy*, 16(2):338–345, 2022.
- Katharine Ricke, Laurent Drouet, Ken Caldeira, and Massimo Tavoni. Country-level social cost of carbon. *Nature Climate Change*, 8(10):895, 2018.
- KC Samir and Wolfgang Lutz. The human core of the shared socioeconomic pathways: Population scenarios by age, sex and level of education for all countries to 2100. *Global Environmental Change*, 42:181–192, 2017.
- Richard Schmalensee and Robert N Stavins. Lessons learned from three decades of experience with cap and trade. *Review of Environmental Economics and Policy*, 2017.
- Falko Ueckerdt, Katja Frieler, Stefan Lange, Leonie Wenz, Gunnar Luderer, and Anders Levermann. The economically optimal warming limit of the planet. *Earth System Dynamics*, 10(4):741–763, 2019.
- Frederick van der Ploeg and Aart de Zeeuw. Non-cooperative and cooperative responses to climate catastrophes in the global economy: A north–south perspective. *Environmental and Resource Economics*, 65:519–540, 2016.
- World Bank. Total greenhouse gas emissions (kt of co2 equivalent), 2020. URL <https://data.worldbank.org/indicator/EN.ATM.GHGT.KT.CE>.

Appendix for Online Publication

A.1 List of Parameters

Table A.1: Key parameters.

Parameter	Description
Economic parameters	
$\beta = 0.985$	Discount factor
$\gamma = 1.45$	Elasticity of marginal utility
$\alpha = 0.3$	Output elasticity of capital
$\delta = 0.1$	Annual depreciation rate of capital
Climate parameters	
$\zeta = 0.0021$	Contribution rate of carbon emissions to temperature
$\sigma_{i,t}$	Carbon intensity (GtC per trillion \$)
$b_{1,i}, b_{2,i}, b_{3,i}, b_{4,i}$	Abatement cost parameters
$\pi_{1,i}, \pi_{2,i}$	Climate damage parameters
TFP parameters	
$g_{i,0}, g_{i,t}$	Growth rate of TFP
d_i	Parameters of TFP growth

A.2 List of Countries

Table A.2: List of countries for regional aggregation.

Region	Constituent Countries
Africa	Algeria, Angola, Benin, Botswana, Burkina Faso, Burundi, Cameroon, Cape Verde, Central African Republic, Chad, Comoros, Democratic Republic of the Congo, Republic of the Congo, Cote d'Ivoire, Djibouti, Arab Republic of Egypt, Equatorial Guinea, Eritrea, Ethiopia, Gabon, Republic of The Gambia, Ghana, Guinea, Guinea-Bissau, Kenya, Lesotho, Liberia, Libya, Madagascar, Malawi, Mali, Mauritania, Mauritius, Morocco, Mozambique, Namibia, Niger, Nigeria, Rwanda, Sao Tome and Principe, Senegal, Seychelles, Sierra Leone, Somalia, South Africa, Sudan, Swaziland, Tanzania, Togo, Tunisia, Uganda, Zambia, and Zimbabwe.
European Union ¹³	Austria, Belgium, Czech Republic, Denmark, Faeroe Islands, Finland, France, Germany, Greece, Greenland, Hungary, Iceland, Ireland, Italy, Luxembourg, Malta, Netherlands, Norway, Poland, Portugal, Slovak Republic, Spain, Sweden, Switzerland, Turkey, and the United Kingdom.
Eurasia	Albania, Armenia, Azerbaijan, Belarus, Bosnia and Herzegovina, Bulgaria, Croatia, Estonia, Georgia, Kazakhstan, Kyrgyz Republic, Latvia, Lithuania, Macedonia FYR, Moldova, Montenegro, Romania, Serbia, Slovenia, Tajikistan, Turkmenistan, Ukraine, and Uzbekistan.
Latin America	Antigua and Barbuda, Argentina, Aruba, Commonwealth of The Bahamas, Barbados, Belize, Bermuda, Bolivia, Brazil, Cayman Islands, Chile, Colombia, Costa Rica, Cuba, Dominica, Dominican Republic, Ecuador, El Salvador, Grenada, Guatemala, Guyana, Haiti, Honduras, Jamaica, Mexico, Netherlands Antilles, Nicaragua, Panama, Paraguay, Peru, Puerto Rico, St. Kitts and Nevis, St. Lucia, St. Vincent and the Grenadines, Suriname, Trinidad and Tobago, Uruguay, Bolivarian Republic of Venezuela, and the U.S. Virgin Islands.

¹³The current EU does not contain the United Kingdom, but in this paper we still assume the United Kingdom is in the EU for convenience.

Region	Constituent Countries
Middle East	Bahrain, Cyprus, Islamic Republic of Iran, Iraq, Israel, Jordan, Kuwait, Lebanon, Oman, Qatar, Saudi Arabia, Syrian Arab Republic, United Arab Emirates, West Bank and Gaza, and the Republic of Yemen.
Other Non-OECD Asia	Afghanistan, Bangladesh, Bhutan, Brunei Darussalam, Cambodia, Fiji, French Polynesia, Indonesia, Kiribati, Democratic People's Republic of Korea, Lao PDR, Malaysia, Maldives, Mongolia, Myanmar, Nepal, New Caledonia, Pakistan, Papua New Guinea, Philippines, Samoa, Solomon Islands, Sri Lanka, Thailand, Timor-Leste, Tonga, Vanuatu, and Vietnam.
Other High-Income	Australia, Canada, Republic of Korea, New Zealand, Singapore.

A.3 Calibration of the TCRE Climate System

Each of the four RCP scenarios (Meinshausen et al., 2011) — RCP 2.6, RCP 4.5, RCP 6, and RCP 8.5 — provide their pathways of emissions, atmospheric carbon concentration, radiative forcing, and atmospheric temperature anomaly. When we calibrate the contribution rate of carbon emissions on temperature, ζ , in a climate system, we use the pathways of emissions and atmospheric temperature anomaly of the four RCP scenarios. Figure A.1 shows that our calibrated TCRE climate system provides a very good projection of the atmospheric temperature anomaly (increase relative to pre-industrial levels) based on cumulative emissions only.

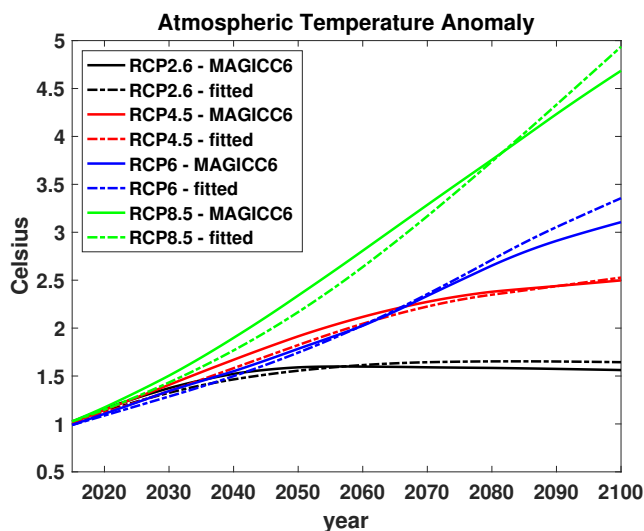


Figure A.1: Calibration of the TCRE climate system.

A.4 Emission Cap Pathways

Figure A.2 shows the regional emission cap pathways generated using the methodology described in Section 5.1. Figure A.3 compares the different emission cap pathways at the global level.

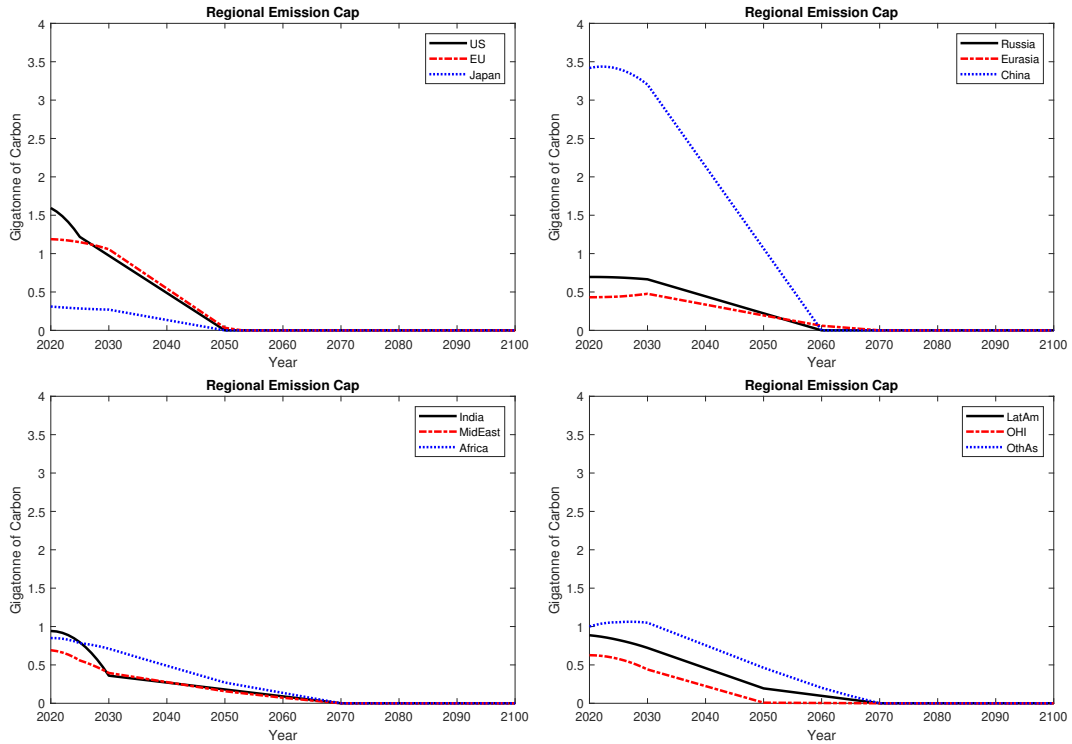


Figure A.2: Regional emission cap pathways under the baseline scenario.

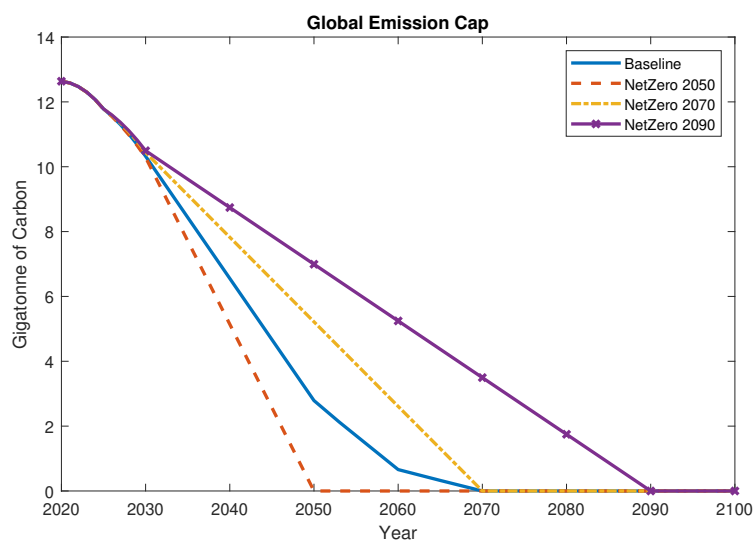


Figure A.3: Global emission cap pathways for the different net zero scenarios.

A.5 GDP Growth Rate beyond this Century

For the GDP growth rate beyond this century, we follow RICE to project $g_{t,i}$ for $t \geq 80$. We begin by assuming the long-run growth rate of TFP in the US is $g_{US,\infty} = 0.0033(1 - \alpha) = 0.00231$ with $\alpha = 0.3$. Next, we let $\tilde{y}_{i,79} = y_{i,79}^{\text{BDD}} y_{i,0} / y_{i,0}^{\text{BDD}}$ be our projected per capita output in 2099, where $y_{i,0}$ is the observed per capita output in 2020. We then assume that the TFP growth in the US is characterized by

$$g_{US,t} = g_{US,\infty} + (g_{US,79} - g_{US,\infty}) \exp(-0.01(t - 79)),$$

and let $\tilde{y}_{US,t+1} = \tilde{y}_{US,t} \exp(g_{US,t}/(1 - \alpha))$ for $t \geq 79$. For the regions other than the US, we assume their TFP growth can be expressed in relation to the TFP growth of the US. Specifically, we assume that, for $t \geq 79$,

$$\begin{cases} \tilde{y}_{i,t+1} = \tilde{y}_{i,t} \exp(g_{i,t}/(1 - \alpha)) \\ g_{i,t+1} = g_{US,t+1} + (1 - \alpha)\chi \ln(\tilde{y}_{US,t}/\tilde{y}_{i,t}) \end{cases}$$

where $\chi = 0.005$ is chosen such that $g_{i,t}$ gradually moves toward $g_{US,t}$ as $t \rightarrow \infty$.¹⁴

¹⁴Assume $\tilde{y}_{i,t} = A_{i,t} k_{i,t}^\alpha$ is GDP per capita where $k_{i,t}$ is capital per capita. We have

$$\ln \left(\frac{\tilde{y}_{i,t+1}}{\tilde{y}_{i,t}} \right) = g_{i,t} + \alpha \ln \left(\frac{k_{i,t+1}}{k_{i,t}} \right).$$

If we assume the growth of $k_{t,i}$ is equal to the growth of GDP per capita, then we have

$$\tilde{y}_{i,t+1} = \tilde{y}_{i,t} \exp(g_{i,t}/(1 - \alpha)).$$

A.6 Calibration of Total Factor Productivity

Figure A.4 shows that with our calibrated $A_{i,t}$, the GDP per capita $y_{i,t}^{\text{NoCC}}$ matches well with the projected data $y_{i,t}^{\text{BDD}}$ from Burke et al. (2018) for all regions.

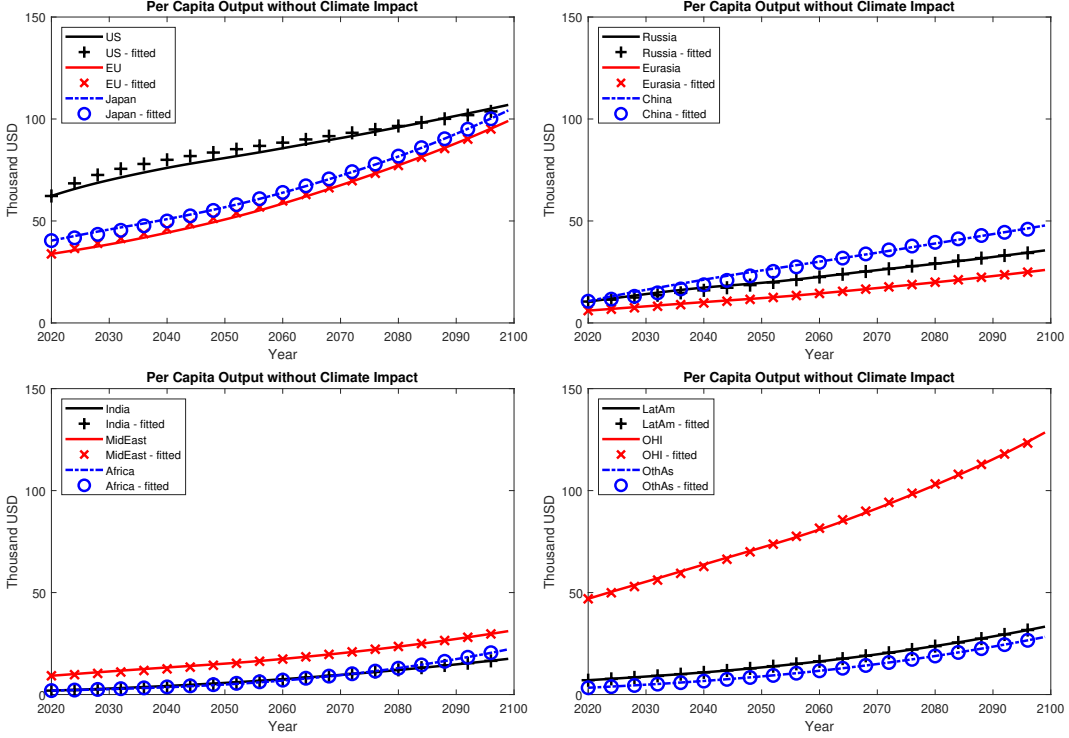


Figure A.4: Fitting GDP per capita under no climate impact. Lines represent GDP per capita from Burke et al. (2018); marks represent fitted GDP per capita.

A.7 Calibration of Climate Damage

Figure A.5 shows that with our calibrated climate damage coefficients, the ratios of GDP per capita between RCP 2.6 and RCP8.5 from our model, matches well with the ratios in Kahn et al. (2021), for every region.

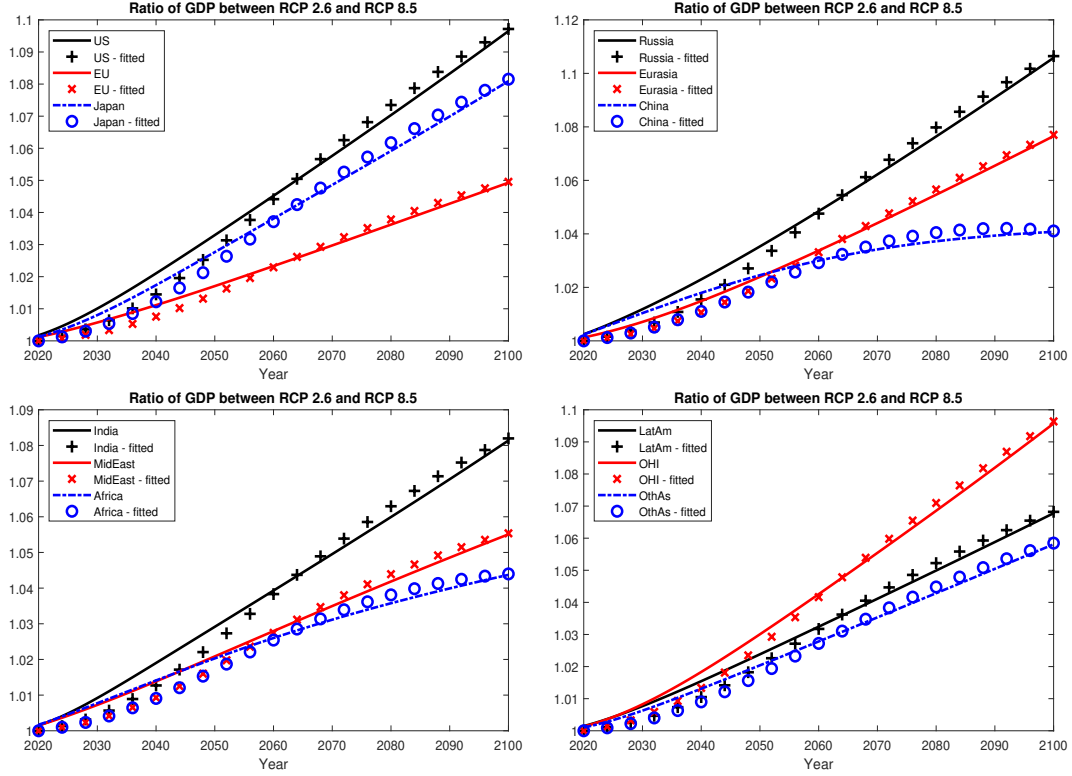


Figure A.5: Fitting climate damage parameters. Lines represent the ratios of GDP per capita between RCP 2.6 and RCP8.5 from Kahn et al. (2021); marks represent fitted ratios.

A.8 Additional Simulation Results

A.8.1 Regional Net Emissions under Noncooperation

Figure A.6 displays the regional net emissions under the noncooperative model with the ETS and the baseline emission cap scenario. Latin America is the first to reach net emissions in 2053, followed by Russia in 2055, the US in 2056, OHI in 2057, and Eurasia in 2058. Then, net emissions are achieved by China in 2061, Japan in 2062, the MidWest in 2064, and the EU in 2065. Finally, India achieves net emissions in 2069, followed by Africa and other non-OECD Asian countries in 2071.

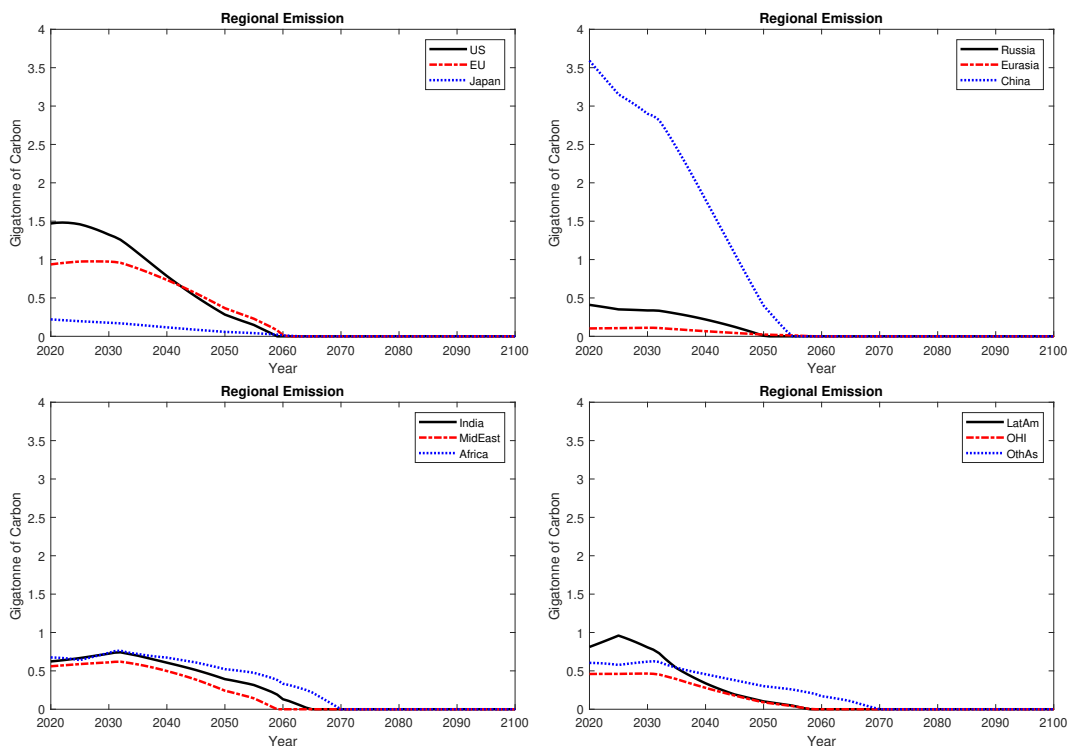


Figure A.6: Simulation results of regional net emissions under noncooperation with the ETS and baseline emission caps.

A.8.2 Regional Net Emissions Comparison between Different Cases

Figure A.7 compares regional net emissions between two cases under cooperation with the baseline emission caps: (i) with the ETS, (ii) without the ETS.

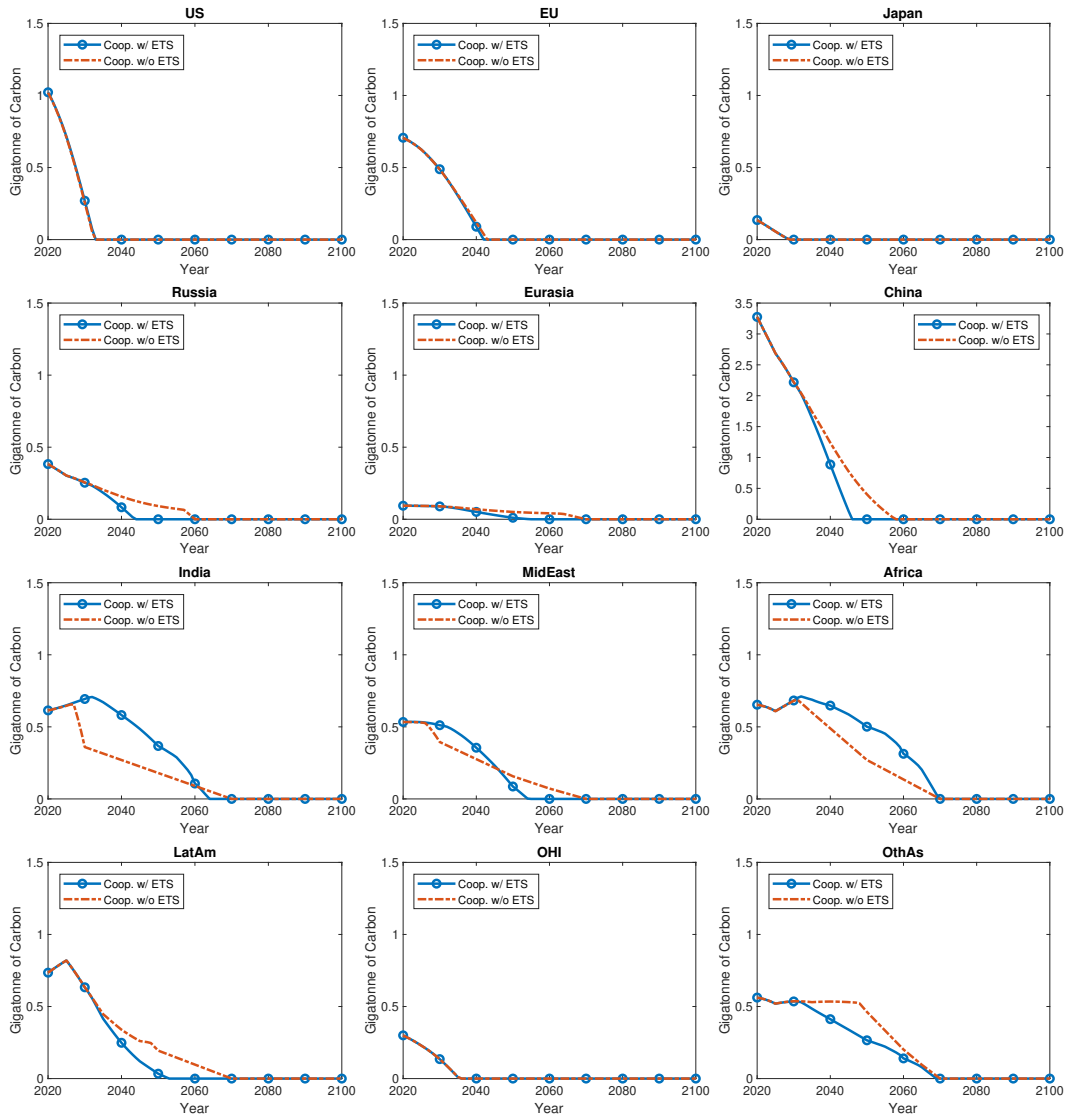


Figure A.7: Simulation results of regional net emissions: comparison between two cases under cooperation.

Figure A.8 compares regional net emissions between two cases under non-cooperation with the baseline emission caps: (i) with the ETS, (ii) without the ETS.

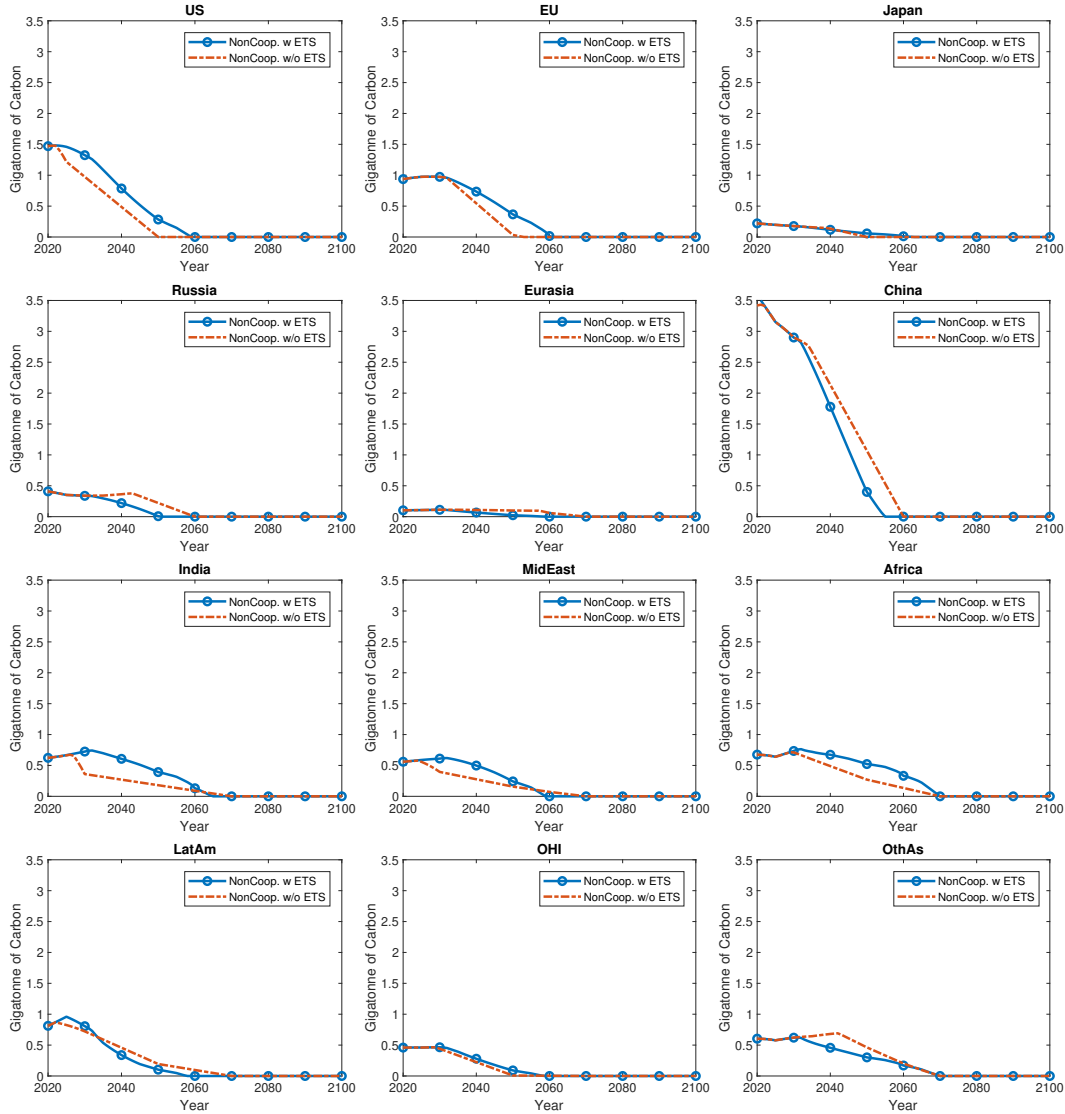


Figure A.8: Simulation results of regional net emissions: comparison between two cases under noncooperation.

A.8.3 Regional MAC Comparison between Different Cases

Figure A.9 compares the regional MAC under cooperation with the baseline emission caps. We compare two cases: (i) with the ETS, (ii) without the ETS.

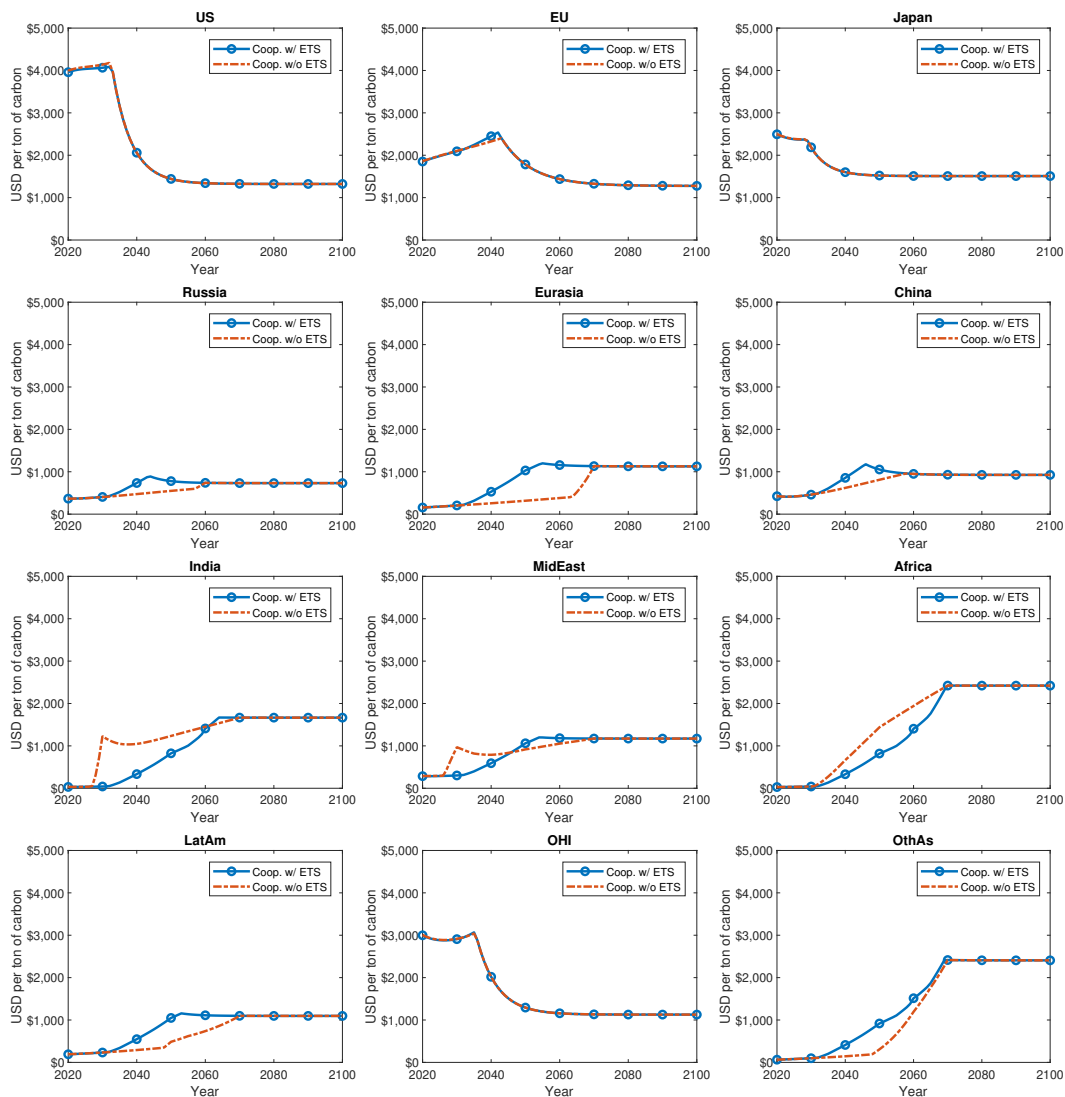


Figure A.9: Simulation results of regional MAC: comparison between two cases under cooperation.

Figure A.10 compares the regional MAC under noncooperation with the baseline emission caps. We compare two cases: (i) with the ETS, (ii) without the ETS.

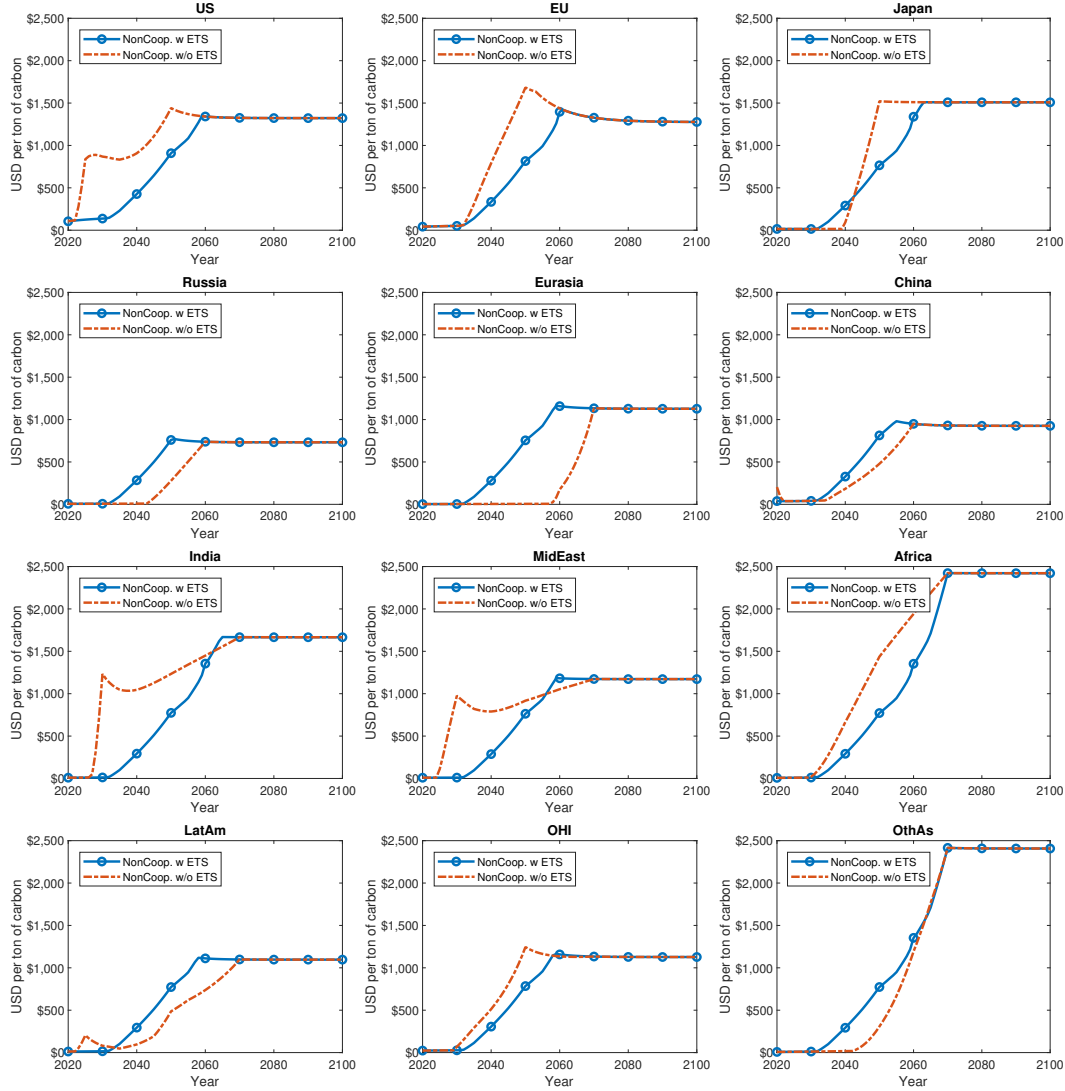


Figure A.10: Simulation results of regional MAC: comparison between two cases under noncooperation.

A.8.4 Regional SCC Comparison between Different Cases

Figure A.11 compares the regional SCC under cooperation with the baseline emission caps. We compare two cases: (i) with the ETS, (ii) without the ETS.

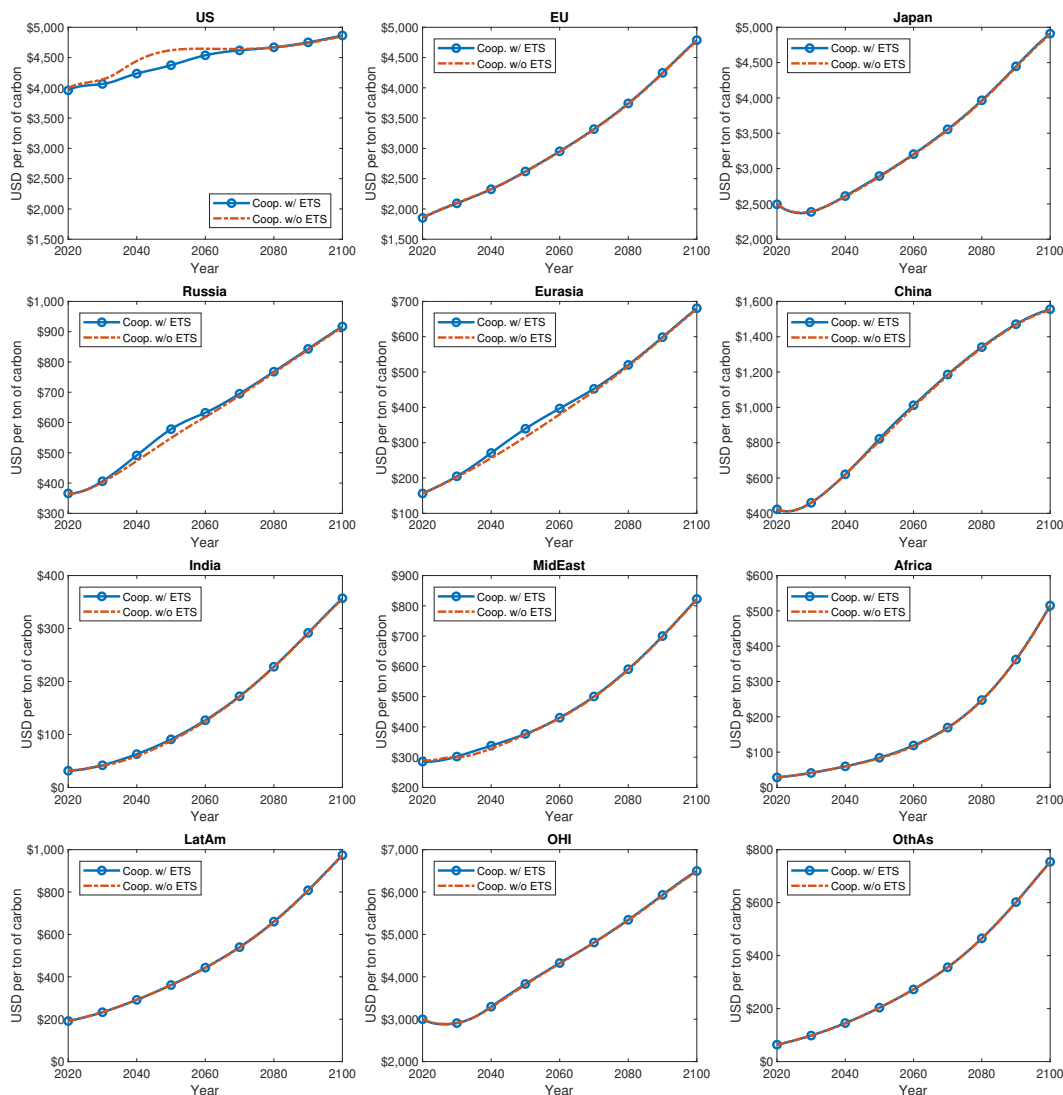


Figure A.11: Simulation results of the regional SCC: comparison between two cases under cooperation.

Figure A.12 compares the regional SCC under noncooperation with the baseline emission caps, comparing two cases: (i) with the ETS, (ii) without the ETS.

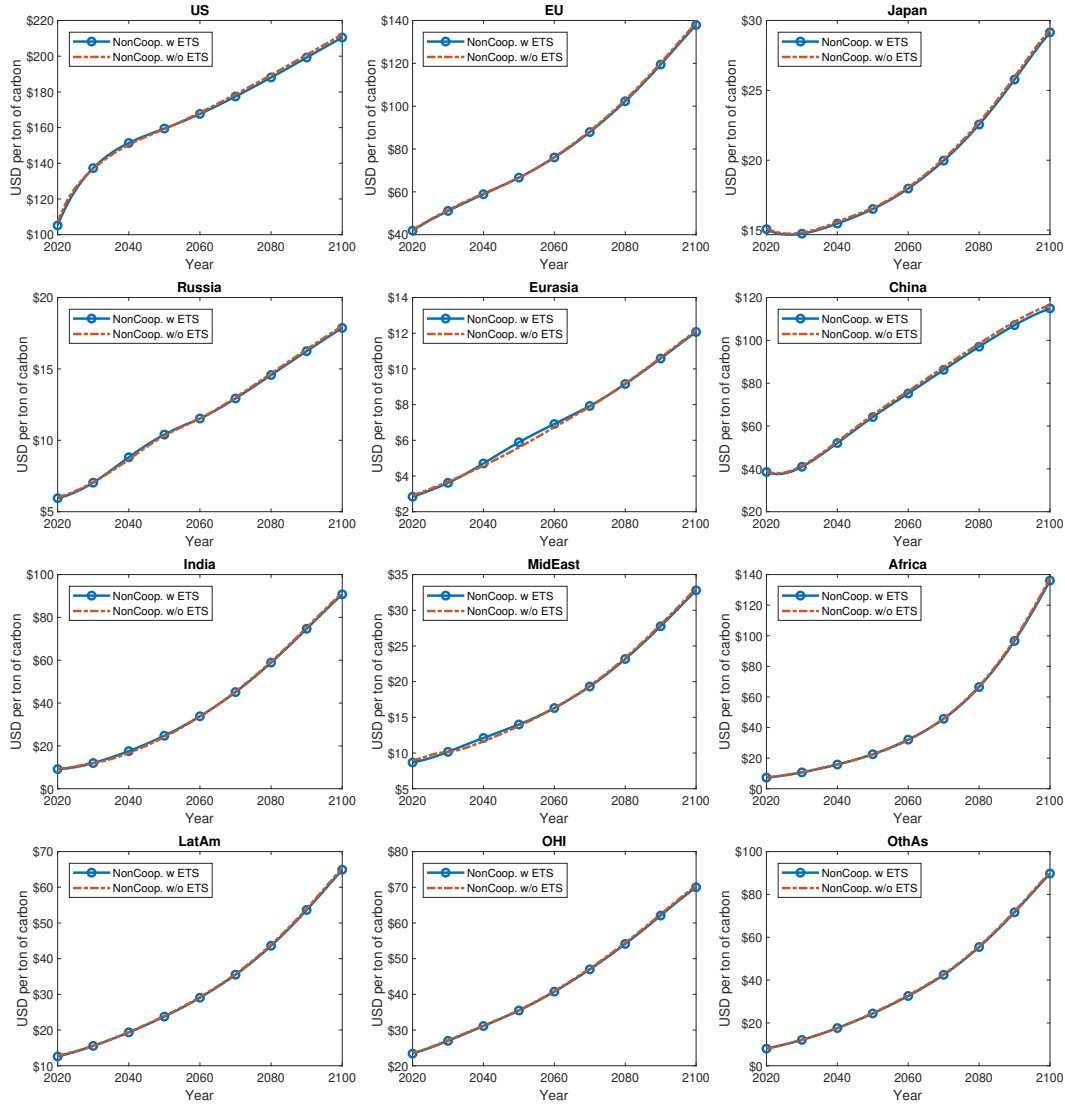


Figure A.12: Simulation results of the regional SCC: comparison between two cases under noncooperation.

A.8.5 Regional MAC and SCC under Alternative Emission Caps

In Figure A.13, we compare the MAC for the noncooperative model with the ETS across alternative emission cap scenarios.

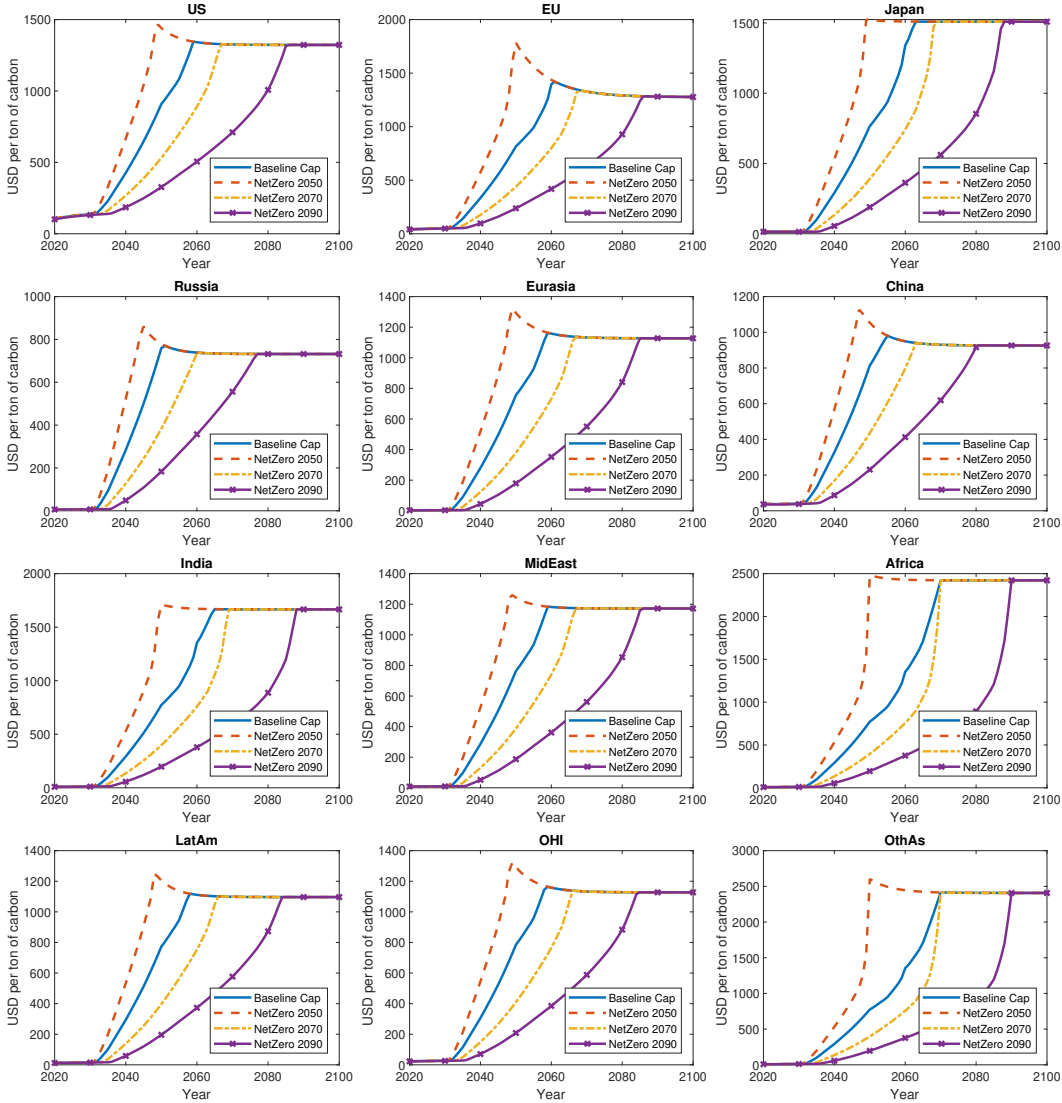


Figure A.13: Simulation results of regional MAC: comparison across alternative emission cap scenarios.

Similarly, Figure A.14 displays the SCC of the noncooperative model with the ETS across different emission cap scenarios.

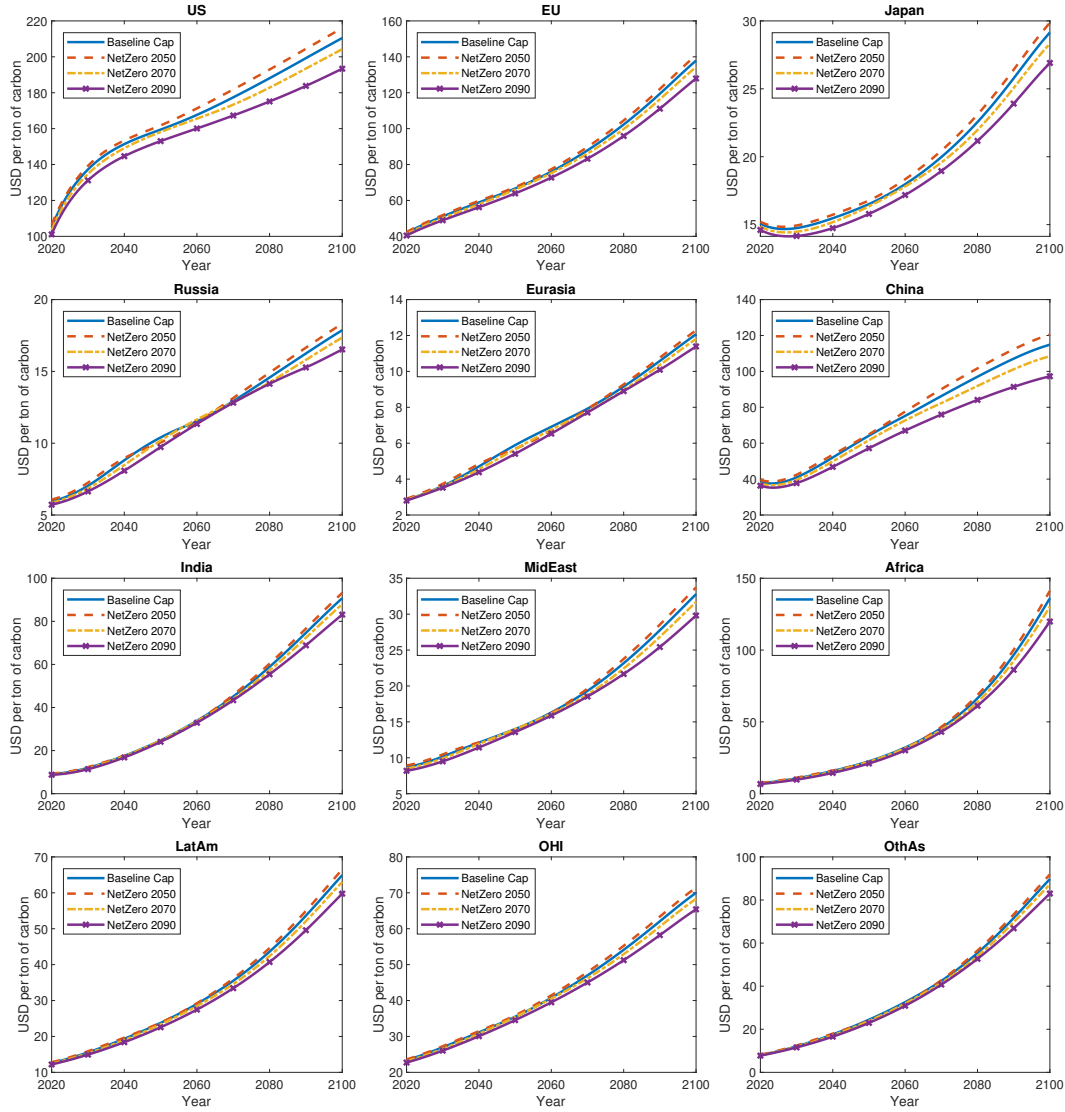


Figure A.14: Simulation results of regional SCC: comparison across alternative emission cap scenarios.